

ลอจิกเกตส์จากบัลค์ออปโตดแบบเลือกจำเพาะต่อไอออนโซเดียมและโพแทสเซียม

นางสาวทรงศิธา สุขสวัสดิ์

วิทยานิพนธ์นี้เป็นส่วนหนึ่งของการศึกษาตามหลักสูตรปริญญาวิทยาศาสตรมหาบัณฑิต

สาขาวิชาเคมี ภาควิชาเคมี

คณะวิทยาศาสตร์ จุฬาลงกรณ์มหาวิทยาลัย

ปีการศึกษา 2553

ลิขสิทธิ์ของจุฬาลงกรณ์มหาวิทยาลัย

LOGIC GATES FROM SODIUM AND POTASSIUM ION SELECTIVE BULK OPTODE

Miss Dhassida Sooksawat

A Thesis Submitted in Partial Fulfillment of the Requirements
for the Degree of Master of Science Program in Chemistry

Department of Chemistry

Faculty of Science

Chulalongkorn University

Academic Year 2010

Copyright of Chulalongkorn University

Thesis Title LOGIC GATES FROM SODIUM AND POTASSIUM ION
 SELECTIVE BULK OPTODE
By Miss Dhassida Sooksawat
Field of Study Chemistry
Thesis Advisor Professor Thawatchai Tuntulani, Ph.D.

Accepted by the Faculty of Science, Chulalongkorn University in Partial
Fulfillment of the Requirements for the Master's Degree

.....Dean of the Faculty of Science
(Professor Supot Hannongbua, Dr.rer.nat.)

THESIS COMMITTEE

..... Chairman
(Assistant Professor Warinthorn Chavasiri, Ph.D.)

..... Thesis Advisor
(Professor Thawatchai Tuntulani, Ph.D.)

..... Examiner
(Assistant Professor Soamwadee Chaianansutcharit, Ph.D.)

..... Examiner
(Assistant Professor Wanlapa Aeungmaitrepirom, Ph.D.)

..... External Examiner
(Wittaya Ngeontae, Ph.D.)

ทรรศิดา สุขสวัสดิ์ : ลอจิกเกตส์จากบัลค์ออปโทดแบบเลือกจำเพาะต่อไอออนโซเดียมและโพแทสเซียม. (LOGIC GATES FROM SODIUM AND POTASSIUM ION SELECTIVE BULK OPTODE) อ.ที่ปริภษาวิทยานิพนธ์หลัก: ศาสตราจารย์ ดร.ธวัชชัย ต้นทุลานี, 77 หน้า.

ลอจิกเกตส์ทางเคมีสร้างจากบัลค์ออปโทดประกอบด้วย tetramethoxyethylester calix[4]arene หรือ valinomycin สำหรับตรวจวัดไอออนโซเดียมหรือไอออนโพแทสเซียม และโครโมไอออนฟอรฺชนิดต่างๆ ในตัวกลางพอลิไวนิลคลอไรด์ กลไกการตอบสนองของออปโทดเป็นสมดุคการแข่งขันของการแลกเปลี่ยนไอออน สัมพันธ์กับระบบลอจิกโดยมีอินพุตสองชนิดคือโปรตอน และ ไอออนโซเดียมหรือโพแทสเซียม เอาท์พุตเป็นสัญญาณเชิงแสงของออปโทดเมมเบรน ได้ศึกษาพฤติกรรมการดูดกลืนแสงของออปโทดเมมเบรนชนิดโซเดียมและโพแทสเซียมในสภาวะที่มีความเข้มข้นต่างๆ ของสองอินพุตอย่างครอบคลุม ระบบบัลค์ออปโทดของโซเดียม และโพแทสเซียมสามารถแสดงลอจิกเกตส์ INH A, INH B, NINH A และ NINH B นอกจากนี้ยังทำการศึกษาระบบออปโทดเมมเบรนที่ประกอบด้วยไอออนฟอรฺที่ไม่มีความจำเพาะในการเลือกจับกับไอออนที่สนใจ (tetramethoxyethylester calix[4]arene- K^+) สามารถแสดงเกตส์ INH และ NINH เช่นเดียวกับกรณีที่ระบบออปโทดเมมเบรนที่ประกอบด้วยไอออนฟอรฺที่มีความจำเพาะในการเลือกจับกับไอออนที่สนใจ แต่มีสภาวะของสารละลายที่แสดงลอจิกเกตส์ทางเคมีน้อยกว่า การสลับค่าลอจิกของอินพุตโปรตอนให้เป็นค่าตรงกันข้ามจากเดิมทำให้ได้ลอจิกเกตส์ชนิดใหม่คือ จากเดิมที่เป็น INH A/NINH A กลายเป็น AND/NAND และจาก INH B/NINH B กลายเป็น NOR/OR ลอจิกเกตส์ นอกจากนี้เกตส์ NOR และ OR ยังได้จากกรณีที่ใช้ระบบออปโทดเมมเบรนที่เป็นไอออนฟอรฺผสม (tetramethoxyethylester calix[4]arene กับ valinomycin) โดยมีอินพุตเป็นไอออนโซเดียม และไอออนโพแทสเซียม เช่นเดียวกับการประมวลผลข้อมูลในระบบอิเล็กทรอนิกส์ ระบบออปโทดเมมเบรนสามารถใช้รวบรวมข้อมูลเหมือนเป็นระบบวินิจฉัยโรคขนาดย่อ และอาจนำไปประยุกต์ใช้ในภาวะร่างกายของสิ่งมีชีวิตได้

ภาควิชาเคมี..... ลายมือชื่อนิสิต

สาขาวิชา.....เคมี..... ลายมือชื่ออาจารย์ที่ปริภษาวิทยานิพนธ์หลัก

ปีการศึกษา.....2553.....

507 22806 23: MAJOR CHEMISTRY

KEYWORDS: BULK OPTODE / LOGIC GATE

DHASSIDA SOOKSAWAT: LOGIC GATES FROM SODIUM AND POTASSIUM ION SELECTIVE BULK OPTODE. THESIS ADVISOR: PROFESSOR THAWATCHAI TUNTULANI, Ph.D., 77 pp.

The optode membranes incorporating tetramethoxyethylester calix[4]arene or valinomycin for sodium ion or potassium ion recognition, respectively and different types of chromoionophores in a plasticized poly(vinyl chloride), (PVC) matrix was fabricated to operate as chemical logic gates. A competitive ion exchange equilibrium, which was the response mechanism, could relate to a logic system under the action of two chemical inputs (H^+ and Na^+/K^+). The response change, an optical character of optode membranes, was the output signal. The absorbance behaviors of sodium and potassium selective optodes at different protonation and coordination environments were studied extensively. Typical optode systems, i.e. sodium and potassium optodes were found to function as INH A, INH B, NINH A and NINH B gates. Mismatched ionophore-analyte ion optodes (tetramethoxyethylester calix[4]arene- K^+) which could partially determine ion contents, also produced INH and NINH gates but not as many conditions as the matched cases. Switching proton input to an opposite logic condition can employ AND/NAND and NOR/OR logic gates from the condition of INH A/NINH A and INH B/NINH B respectively. NOR and OR gates were achieved from the modified mixed-ionophore optode systems (tetramethoxyethylester calix[4]arene and valinomycin) with Na^+ and K^+ as inputs. As well as processing information, our system could be used for information gathering as a miniaturized diagnostic system capable of working under physiological conditions.

Department:Chemistry..... Student's Signature

Field of Study: ...Chemistry..... Advisor's Signature

Academic Year:2010.....

ACKNOWLEDGEMENTS

I wish to express highest appreciation to my thesis advisor, Prof. Dr. Thawatchai Tuntulani, for his valuable guidance, understanding and patience. My deepest thanks would be expressed to Dr. Wittaya Ngeontae for his beneficial advice and encouragement which had a great benefit through my thesis work. I am also grateful to Asst. Prof. Dr. Warinthorn Chavasiri, Asst. Prof. Soamwadee Chaianansutcharit, Asst. Prof. Dr. Wanlapa Aeungmaitrepirom for their valuable suggestions and comments as committee members and thesis examiners.

This thesis cannot be complete without kindness and helps from many people. I would like to thank the Supramolecular Chemistry Research Unit and Environmental Analysis Research Unit for the facilities. The friendship and support from two group members are invaluable. I wish to express my sincere thanks to Miss Wanwisa Janrungroatsakul, Miss Wassamon Phusakulkajorn, Miss Paramita Phanwong and Miss Jitwilai Waluwanaruk for their helpful recommendations and encouragement.

Recognition would be expressed to the Development and Promotion of Science and Technology Talent Project (DPST) and Center of Petroleum, Petrochemicals, an Advanced Materials for the financial support through my graduate study.

Thanks to my family for their love, support and encouragement.

CONTENTS

	PAGE
ABSTRACT (IN THAI)	iv
ABSTRACT (IN ENGLISH).....	v
ACKNOWLEDGEMENTS	vi
LIST OF TABLES	ix
LIST OF FIGURES	x
LIST OF ABBREVIATIONS.....	xii
CHAPTER I INTRODUCTION	1
1.1 Research Objective	2
1.2 Scope of the Research	2
1.3 Benefits of the Research	3
CHAPTER II THEORY AND LITERATURE REVIEWS	4
2.1 Molecular Logic Gates.....	4
2.2 Computing in Molecular System	6
2.3 Optodes	21
CHAPTER III EXPERIMENTAL	27
3.1 Apparatus	27
3.2 Chemicals.....	27
3.3 Membrane Preparation.....	30
3.4 Logic Gate Preparation	31
3.5 Threshold Value for Absorbance Output	31
CHAPTER IV RESULTS AND DISCUSSION	32
4.1 Matched ionophore-primary ion	32
4.2 Mixed ionophore-2-primary ion.....	44
4.3 Mismatched ionophore-primary ion.....	46
CHAPTER V CONCLUSIONS.....	51
REFERENCES	53

	PAGE
APPENDICES	61
Appendix A Digital System Organization.....	62
Appendix B Logic Gates	64
Appendix C Boolean Algebra	69
Appendix D Threshold Value for Absorbance Output Calculation.....	72
Appendix E Details of Non-Logic Gate Operations	74
VITA.....	77

LIST OF TABLES

TABLE		PAGE
3.1	Chemicals list.....	28
3.2	The amount of components in optodes	30
4.1	Wavelength for outputs O1 and O2	33
4.2	Truth table corresponding to INH/NINH A and B gates	36
4.3	pHs and metal concentrations which operated INH, NINH, AND, NAND, OR and NOR logic gates for sodium optodes	39
4.4	pHs and metal concentrations which operated INH, NINH, AND, NAND, OR and NOR logic gates for potassium optodes	39
4.5	Truth table corresponding to AND/NAND and OR/NOR gates	43
4.6	Truth table corresponding to OR/NOR gates.....	46
4.7	pH value operated OR/NOR logic gates for mixed ionophore optode with sodium and potassium ions	46
4.8	pH and metal concentration operated INH, NINH, AND, NAND, OR and NOR logic gates logic gates for sodium optode with potassium ion	47
5.1	Logic gates derived from studied bulk optodes systems	51

LIST OF FIGURES

FIGURE		PAGE
2.1	Input and output channels of molecular logic devices.....	5
2.2	Principle of a PET chemically driven luminescent molecular switch	8
2.3	Structure of 1	9
2.4	Molecular systems corresponding to OR gate	12
2.5	Structures of compounds 4 , 5 and 6	13
2.6	Structure of molecular system 7	14
2.7	Schematic representation of the unthreading/rethreading pattern of pseudorotaxane 8 , which corresponds to an XOR logic function.....	15
2.8	Molecular structures of 11 , 12 and 13 which can undergo INH logic operations.....	17
2.9	Structures of inverted logic gate molecules 14-20	19
2.10	Structures of reconfigurable and superimposed molecular logic devices 21 and 22	21
2.11	Schematic representation of a pH optode based on an anionic indicator dye directly immobilized on the surface of the optical element.....	22
2.12	Neutral-carrier-based optodes with neutral or charged chromoionophores.....	24
3.1	Major components of sodium/potassium selective optodes...	29
4.1	Phase transfer equilibrium of neutral-carrier-based optode...	33
4.2	Absorbance features of protonated and deprotonated wavelength using studied chromoionophores.....	34
4.3	Absorbance features of the INH A and NINH A gates of sodium optode of studied chromoionophores	36
4.4	Absorbance features of the INH B and NINH B gates of sodium optode of studied chromoionophores	37

FIGURE		PAGE
4.5	Bar diagram featuring the logic operation of the optical systems	38
4.6	Absorbance features of the INH A/NINH A and INH B/NINH B gates of potassium optode of studied chromoionophores.....	40
4.7	Symbol for INH A, INH B, AND and NOR gates.....	41
4.8	Interchanges from an INH A gate to an AND gate.....	42
4.9	Interchanges from an INH B gate to an OR gate	44
4.10	Absorbance features of OR and NOR gates using mixed ionophore strategy.....	45
4.11	Absorbance features of the INH A/NINH A and INH B NINH B gates of sodium optode with potassium ions of studied chromoionophores	49

LIST OF ABBREVIATIONS

a_H	=	Proton activity
a_I	=	Sample ion activity
A_D	=	Absorbance of the nonprotonated form of the chromoionophore
A_P	=	Absorbance of the fully protonated form of the chromoionophore
α	=	Normalized absorbance, degree of deprotonation
β_{ILn}	=	Stability constant for ion-ionophore complex
C	=	Chromoionophore
DOS	=	Bis(2-ethylhexyl)sebacate
INH	=	Inhibit
ISE	=	Ion selective electrode
k_H	=	Relative lipophilicity of H^+
k_I	=	Relative lipophilicity of I^{Z+}
K_a	=	Acidity constant for the chromoionophore
K_{exch}^{ILn}	=	Exchange constant
KTpCIPB	=	Potassium tetrakis[4-chlorophenyl] borate
L	=	Ionophore
mmol kg ⁻¹	=	Millimol per kilogram
NAND	=	Not AND
NINH	=	Non-Inhibit
NOR	=	Not OR
PET	=	Photoinduced electron transfer
PVC	=	Poly(vinyl chloride)
R ⁻	=	Cation exchanger
THF	=	Tetrahydrofuran
XNOR	=	Exclusive-NOR
XOR	=	Exclusive-OR

CHAPTER I

INTRODUCTION

The rapid improvement in information processing technology based on silicon devices which all aspects were influenced by miniaturization is unprecedented in the history of technology. Soon the integration scale of electronic components will reach its physical limits and further acceleration will not be possible [1]. A new way to relieve the problem is the application of single molecules and molecular systems for data acquisition, storage, transfer and processing [2]. Although molecular information processing does not necessarily need to follow the semiconductor blueprint, a number of groups have been working on the design, synthesis and characterization of chemical systems that mimic the operation of Boolean logic gates and circuits. During a few decades, many new approaches toward designing advanced molecular logic gates have emerged, ranging from host-guest interactions, coordination chemistry, and self-assemble systems to bioinspired networks [3-10]. The principle of the operation of chemical logic gates is identical to those of electronic logic gates. The input and output signals may have only two values: 0 (OFF, FALSE) or 1 (ON, TRUE). The output signal is a Boolean function of the input signals. Chemical logic gates consist of molecules that can exist in at least two different states (isomers, rotamers, etc.) and there are defined physical or chemical stimuli capable of switching the system from one state to the other (e.g. light, redox potential, temperature, pH, metal ions, etc.). Usually in one chemical system, different attribution of logic variables results in different logic functions [11]. A number of examples for individual molecular logic systems which demonstrate basic logic gates (YES, NOT, AND and OR) and rather complicated two-integrated logic functions such as INH, XOR, NOR, XNOR, NAND gates are available in the literature [12-25]. Despite broadly and encouraging recent progress, a number of technical challengers must be overcome to make readily designable, robust, and universal logic circuit integrated on the molecular scale [26]. More advanced ways to integrate relatively simple logic systems into higher-level devices are still being explored by chemists.

Ion selective optodes have been developed in recent decades. They also were used to successfully measure several clinically important ion species such as Na^+ , K^+ , Ca^{2+} and Cl^- [27-29]. Most of the optical transduction systems of these optodes are based on the measurements of UV-vis absorptions and fluorescence emissions of chromoionophores. The response range is conveniently tunable by adjusting the degree of protonation of the chromoionophore at equilibrium, which is a function of the lipophilicity of the ion, the charge, the basicity of the chromoionophore, and the sensor composition as well as the sample pH. This unique characteristic of bulk optode sensors is important and of great advantage in dealing with samples with drastic changes in the analyte ion or with a large pH range [30-32]. A conventional ion selective optode contains an ionophore L, which selectively forms a complex with a primary metal ion I^{z+} (Na^+/K^+ in this study) and a chromoionophore C, a lipophilic dye, that interacts with a reference ion (H^+) and changes optical properties upon protonation, the third additive is a lipophilic cation-exchanger. Because the concentration of ion-exchanger in the polymer matrix is limited, the competition between two ions (Na^+/K^+ and H^+) for the ion-exchange sites affects the fraction of protonated chromoionophore CH^+ and determines the sensor response [33].

For a new generation of molecular logic gates, we focused on preparing bulk optode logic gates. An optode system can possibly be studied in term of chemical logic gate with 2 inputs: pH and a target metal ion. The response change, an absorbance, is the output signal.

1.1 Research Objective

This research aims to obtain chemical logic gates utilizing an optode response mechanism.

1.2 Scope of the Research

The optode membranes incorporating tetramethoxyethylester calix[4]arene or valinomycin for sodium ion or potassium ion recognition, respectively and different types of chromoionophores and lipophilic cation exchanger in a plasticized poly(vinyl chloride) (PVC) matrix were prepared. The neutral H^+ -selective chromoionophores

used in this study were Nile Blue derivatives (chromoionophore I, ETH 5294; chromoionophore VII, ETH 5418; and Nile Blue-urea) and a acridine derivative (chromoionophore XIV). An optical response of optode membranes was an output signal. The absorbance behaviors of sodium and potassium selective optodes at different protonation and coordination environments were studied extensively.

1.3 Benefits of the Research

We expected to obtain all possible two-input logic gates mimicking computing networks from sodium and potassium selective bulk optodes. Moreover, our proposed systems could be used for determining the predominant ion in the suspicious solution.

CHAPTER II

THEORY AND LITERATURE REVIEWS

2.1 Molecular Logic Gates

The concept of binary logic is, however, general and can thus be extended to any type of signal, including chemical, optical, and mechanical. Of course, devices are needed to respond to such signals according to the logic gate rules.

It is not necessarily that the compounds of a molecular computer will have to operate in ways analogous with those of conventional silicon-based computers, much effort has been devoted to the design, synthesis, and characterization of molecular systems in which silicon-based logic can, in principle, be mimicked. It is worth noting that each encoding scheme will bring with it a set of advantageous features if we can choose appropriate applications for it.

Molecular information processing is a common feature of numerous biological and chemical systems. Living things have always processed information for purposes of survival. [34] All of the regulatory processes in living cells, cellular signaling, and of course all of the neurobiological activities process information at the molecular level. Every biochemical bifurcate pathway undergoes Boolean logic rules at the molecular level in a sense that every single molecule can follow only one reaction path: therefore, its fate can be described in terms of Boolean algebra.

The whole spectrum of input and output data encoding channels (Figure 2.1) should be considered. Classical electronic devices use electronic input/electronic output communication, but any other combination is possible. Biological systems utilize various chemical stimuli for communication, while artificial systems use all possible combinations of input and output channels.

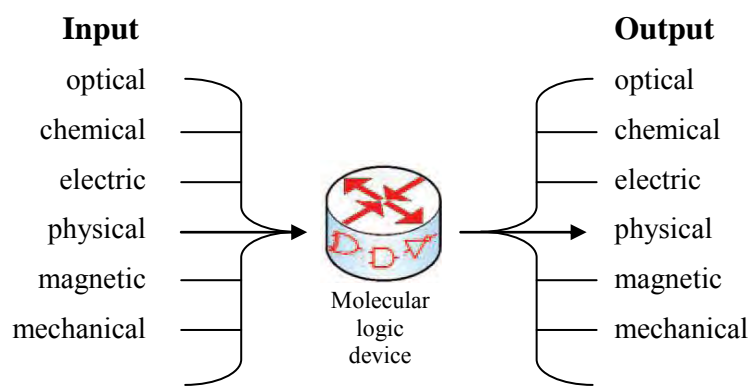


Figure 2.1. Input and output channels of molecular logic devices. These devices can be based on classical electronics paradigms (electronic input/electronic output) or utilize any nonclassical input/output configurations. [35]

In principle, any chemical system that can exist in two quasi-stable states of different chemical or physical properties may be regarded as a molecular switch (or molecular logic gate) provided there are some physical or chemical stimuli that can (reversibly) change the state of the system. The simplest examples are colorimetric pH indicators, compounds changing their color upon changes in proton concentration. They function as YES or NOT logic gates, depending on the property of the individual indicator and the assignment of input and output channels (e.g., pH values and colors). Furthermore, they are molecular devices that enable information transfer from the molecular level (presence of target molecules, e.g., protons) to the macroscopic level (observable change of optical properties). In order to perform any useful calculations, the switching process should be based on reversible chemical processes. [35] Only then might the switches „talk“ to each other or to other devices in a circuit. In most prototype molecular logic gates, the output is optical: an input signal alters the molecule’s light emission or absorption properties.

As well as thinking more deeply about computer architecture, molecular logic researchers will need to address some fundamental obstacles inherent to the technology. Intensive interconnection of basic elements to create complex circuits is a distinctive feature of electronic circuits, but constitutes a critical problem for molecular logic elements because in most cases the input and output signals are physically inhomogeneous and hence incompatible. More advanced ways of an

integration of the relatively simple logic systems into higher-level devices are still being exploited by chemists. Despite the apparent disutility of numerous molecular logic systems, their development is a great advance of science. First electronic logic devices were also rather impractical, but in a short time, they became inherent elements of everyday life. In the future, the same may happen with molecular devices. At the moment, numerous information-processing molecules, such as fluorescent sensors, are commonly used in medical diagnostics, environmental analysis, and industry. Furthermore, studies on information processing in molecular systems (not necessarily with single molecules) may lead in the future to a better understanding of the human brain and nervous system operation.

2.2 Computing in Molecular Systems [35]

2.2.1 Simple Molecular Switches

Any chemical system that can exist in at least two forms of different spectral, electrochemical, or magnetic properties can be regarded as a molecular switch. Moreover, these forms should be relatively stable, and the transition of one into the other should not proceed spontaneously, but only upon stimulation with chemical, optical, electrical, or magnetic perturbation. If one state of the switch is assigned to logical 0 (ON) and the other to logical 1 (OFF), the switch should be regarded as one input logic gate: YES or NOT, depending on the state assignment and switching characteristics. The physicochemical processes behind may be very different: energy level rearrangement upon protonation/deprotonation, geometrical isomerization, proton transfer, changes in electron distribution (valence isomerism), spin state changes, bond formation/cleavage, which are the consequence of chemical reactions, photoexcitation, oxidation/reduction, or specific interactions with ions and molecules.

In order to consider a chemical system as a molecular switch, the two states must be easily distinguishable. In the case of fluorescence monitoring, the quantum yield should change from very small ($\Phi \ll 1$) to high ($\Phi \approx 1$), and in the case of absorbance monitoring, the spectral changes should be significant, and the

shift of the absorption (or emission) band should be significantly larger than the corresponding band half-width. The same concerns changes in redox potentials, magnetic properties, or other physicochemical features of molecular systems.

2.2.1.1 Chemically Driven Molecular Switches

Numerous chemically driven molecular switches can be derived from chemosensors. They are molecules or molecular systems changing their optical or electrical properties upon interacting with small anions, cations, or neutral molecules. The use of fluorescence is the most popular due to very high sensitivity and relatively low price of measurement. They are the simplest tools that can transmit information on events occurring at a molecular scale to the macroscopic world.

Chemically driven molecular switches usually comprise three main building blocks: receptor moiety, linker (spacer), and the reporter moiety. Receptor moieties are specially designed for complexing ions or molecules. They should exhibit desirable selectivity and sensitivity toward selected ions. The linker, in turn, should provide electronic communication between the receptor and reported moieties.

The reporter moieties in turn should significantly (*vide supra*) change their photophysical, electrochemical, magnetic, or chemical properties to yield an easily recognizable signal. There are numerous review papers devoted to chemical sensors and switches

Chemical switches with optical readout are usually based on the following photophysical phenomena: photoinduced electron transfer (PET, Figure 2.2), photoinduced charge transfer (PCT), electronic energy transfer (EET), excimer/exciplex formation, and reorganization of electronic structure of transition metal based chromophore/fluorophore.

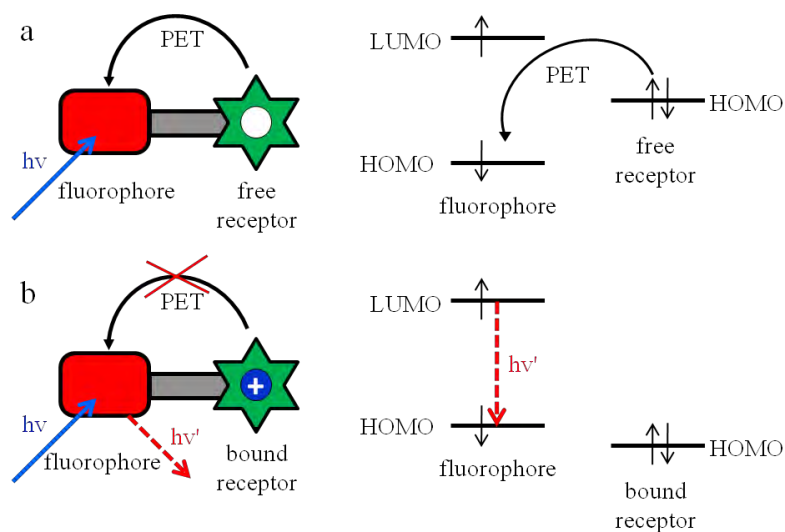


Figure 2.2. Principle of a PET chemically driven luminescent molecular switch. The HOMO level of the unbound receptor acts as an electron donor and effectively quenches the fluorescence of the receptor (a). Upon coordination of the substrate, the energy of the HOMO level of the receptor is decreased because of electrostatic interaction with cationic species, and PET quenching is no longer possible (b).

In the simplest case, the change of the energies of the system is caused by electrostatic and electronic interactions between the receptor and the substrate. Most of the PET switches triggered by protons or closed shell cations work in OFF/ON fashion (i.e., fluorescence is switched on upon binding of the trigger), careful design of the receptor-fluorophore systems also gave the ON/OFF switch. **1** is designed to have no (or weak) PET to the fluorophore from either receptor when they are bound to their appropriate ion (amine/ H^+ and benzo-15-crown-5 ether/ Na^+). This is the “on” state of fluorescence. When the amine group is proton-free, it serves as an efficient PET donor to the fluorophore which is separated by only a methylene group. When protons are presented in a sufficient concentration and Na^+ is absent, the protonated aminomethyl moiety behaves as an electron-withdrawing group on the anthracene fluorophore which permits rapid PET from the benzocrown ether moiety a short distance away. [36]

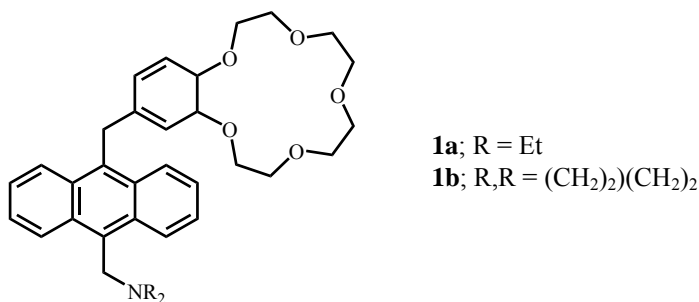


Figure 2.3. Structure of **1**

2.2.1.2 Light Driven Molecular Switches

There is a plethora of well characterized chemical systems in which switching between two, more or less stable, states can be achieved via optical excitation.

Three main photochemical processes should be considered in the context of light-driven molecular switches: photoisomerization of molecules with double bonds, light-induced ring opening and ring-closure reactions, and photoinduced electron transfer. The latter may result in valence tautomerism, which is the basic platform for various magnetic devices or translocation of components of a supramolecular assembly due to PET-induced changes in affinity of the components. The first two phenomena are usually associated with photochromic systems. Photochromism is defined as a reversible phototransformation of a molecule between two forms of different spectral properties. This process, however, may bring about other, not only spectral changes, e.g., refractive index, dielectric constant, dipole moment, oxidation/ reduction potential, or geometry of a molecule. The reverse transformation may proceed upon excitation with light of different wavelength, on thermal pathway or in redox processes.

2.2.1.3 Redox Driven Molecular Switches

Electrochemically driven molecular switches are another large class of molecular systems with prospective application for information processing. There are numerous chemical systems in which the changes in optical properties

(absorption, fluorescence) or molecular geometry/conformation can be controlled and/or switched by redox reactions. There are three main categories of electrochemically switchable molecular systems: supramolecular assemblies in which translocation of molecular fragments is induced by electrochemical processes, electrochemical control over photoinduced energy/electron transfer, and electrochromic switches.

The supramolecular light-driven molecular switches based on donor-acceptor building blocks can be also addressed electrochemically: selective oxidation/reduction of some components results in identical changes in the supermolecule geometry. There are two main classes of electrochemically active compounds, which show geometrical/ topologic changes upon oxidation/reduction. The first class encompasses various transition metal complexes containing two different sets of donor atoms within one supramolecular assembly. Upon change in oxidation state of the central metal ion, the geometry of the supermolecule rearranges to achieve the most favorable coordination environment around the metal ion.

2.2.1.4 Magnetic Switches

Magnetic phenomena were one of the first bases for information storage in electronic devices. Recent development of coordination chemistry, material science, and nanotechnology resulted in new magnetic materials of prospective application in information storage and processing. The most promising are the materials showing the spin crossover (SCO) phenomenon. Magnetic properties the SCO systems can be switched on and off upon thermal, optical, mechanical, or magnetic stimulation.

2.2.1.5 Multistate Molecular Switches

It is possible, however, to find molecular systems that respond to stimulation in a more complex fashion. These molecules and molecular systems can exist in more than two distinguishable stable states and can, therefore, be related to multivalued logic systems. These multistate switches may be based on

multichromophoric photochromic compounds, molecules undergoing orthogonal photochemical and electrochemical switching, supramolecular assemblies with equivalent or nonequivalent redox centers, fluorescence sensors capable of binding more than one target substrate or rotaxanes, and catenanes with a higher number of stations.

2.2.2 Two Input Chemical Logic Gates

The idea of computation at the atomic or molecular level was first mentioned by Richard Feynman in 1959. [37] It took over 30 years for the first practical implementation of Feynman's ideas; the first molecular machines were reported in 1992 by Vincenzo Balzani and co-workers. [38] The work by Balzani et al. describes the first molecular devices based on molecular recognition and self-assembly. Nowadays, rotaxanes and catenanes are elements of molecular logic gates and nanoelectronic devices. Only a year later the first molecular logic gate was reported by A. Prasanna de Silva. [4] The first logic gate has emerged from fluorescent probes based on molecular recognition of target molecules. [39-42] These gates and other devices were controlled exclusively by chemical signals, while the output was observed as changes in fluorescence and absorption spectra. During the last dozen or so years, great progress in the field of molecular logic gates was achieved. There are hundreds of chemical systems that are capable of complex information processing at the molecular level. Information can be fed in as chemical, optical, or electrical signals, while the result is retrieved in most cases as optical or electric signals.

OR Gates

The OR gate, which computes the logic sum of two input variables, is the easiest to be implemented in molecular systems. The OR logic was first recognized in non-selective Na^+/K^+ sensors. [4] Other examples based on the same principle have been reported [43, 44]. A well-behaved OR gate should have the same high level of output when switched on. The example shown in Figure 2.4a refers to cryptand **2** which bears three anthracene units. In THF the fluorescence quantum yield of **2** (10^{-5} M) is very low (0.001, including some exciplex fluorescence) because of

PET from the tertiary nitrogen atoms to anthracene. In the presence of 10^{-2} M Cu^{2+} or Ni^{2+} , the quantum yield increases approximately 100 folds [45, 46]. Another common molecular-level OR gate has been provided [47] (Figure 2.4b), whereby the quantum yield of intramolecular photodimerization of two anthracene moieties is considered as the output. Quantum yield enhancement originates from the guest-enforced steric changes upon binding ions (Na^+ and Hg^{2+}) at either or both available sites (the 2,2'-bipyridine site or the flexible oligooxyethylene chains), giving an orientation conducive to photodimerization. Reset is possible in this instance by ion sequestration followed by irradiation at a rather short wavelength.

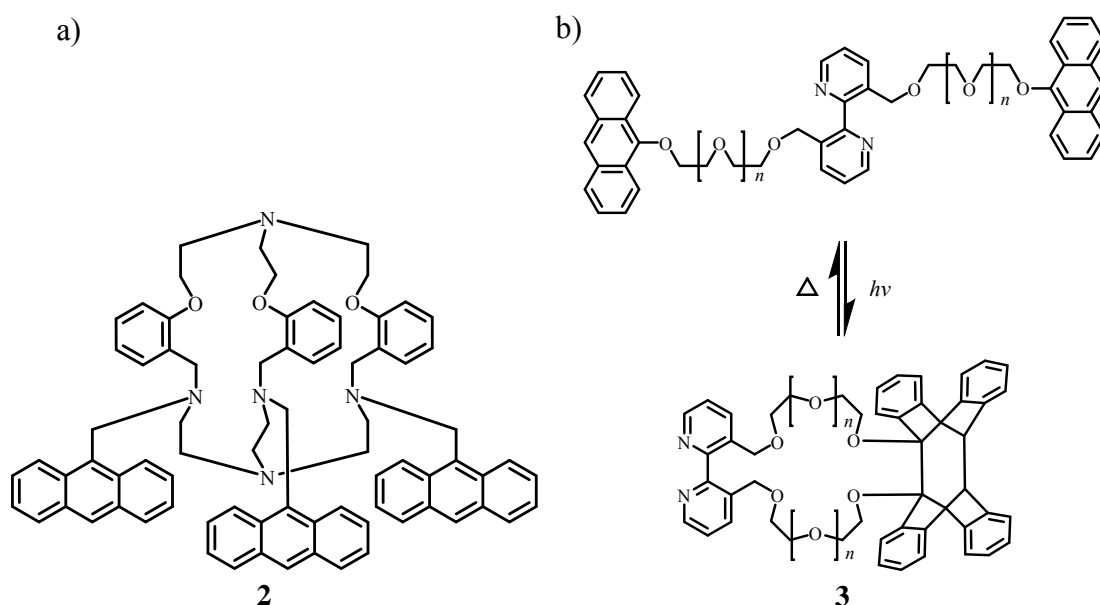


Figure 2.4. Molecular systems corresponding to OR gate

AND Gates [34]

Most of the molecular AND logic gates are based on ditopic receptors and a fluorescent unit linked covalently with both receptors. A molecular-scale, **1** (Figure 2.3) and its predecessor, which used a different arrangement of the constituent modules, are designed through the elaboration of the modular “fluorophore-spacer-receptor” format. This AND gate is made possible by utilizing two discrete, selective binding sites that are weakly coupled to a fluorophore. Thermodynamically controlled and guest-modulated PET processes from oxidizable moieties located at each receptor serve to quench the fluorescence from the excited

fluorophore, across inert methylene spacers. Chemical species (Na^+ and H^+) are present at both receptor₁ and receptor₂, and both oxidation potentials rose, such that the electron transfer is abated. Then the fluorescence output is restored (output 1). In this implementation, the power supply was provided excitation light, while inputs are chemical (Na^+ and H^+) and the output is fluorescence light. Importantly, the commutative nature of this system is apparent as binding of each guest is truly independent. Such photoionic systems can be considered wireless, since the inputs are directed to the correct receptor of the gate unaided, while the photons also find their way in and out of the fluorophore component.

Multi-receptor “fluorophore-spacer-receptor” PET systems showing AND logic can employ chemical species that are more complex than atomic ions. Cooper and James report a system targeting a diol (with boronic acid) and an ammonium ion (with an azacrown ether). The end-result is a selective sensor for glucosamine at physiological pH. [48]

A different example of an AND logic gate with light and chemical inputs and absorbance/fluorescence output is Balzani and Pina's **4** [49]. Diederich's work is also related [50]. The thermodynamically stable *trans*-form **4** is converted to the *cis*-isomer **5** under irradiation (light input 1). Compound **5** is subsequently cyclized to **6** in the presence of H^+ (chemical input 1). Compound **6** is the absorbing/fluorescent species (output 1) and cannot be produced by photoirradiation or H^+ alone.

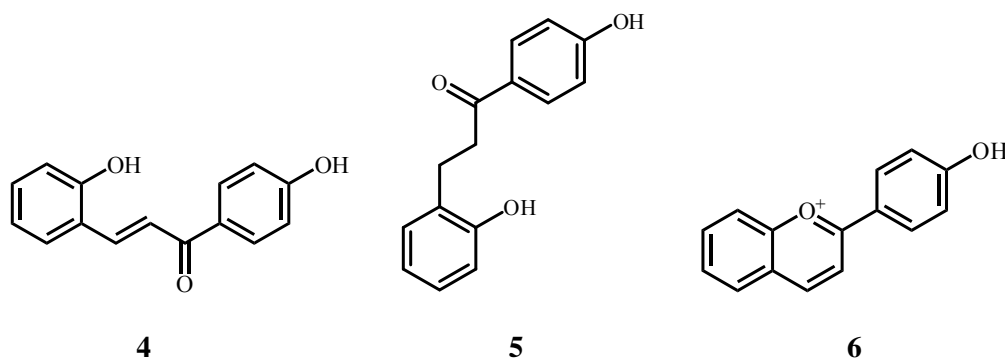


Figure 2.5. Structure of compounds **4**, **5** and **6**

Recent examples of all-optical AND logic gates are from groups of Wasielewski, Levine and Zhang [51-53]. The multi-chromophore system **7** uses pump laser beams of two colors as the two inputs. The output is taken as the absorption of benzenediimide radical anion monitored at a third wavelength. Thus the output employs a negative logic convention, since a high light output will have a low absorbance. The aminonaphthalimide module is pumped (input₁ 1) to cause PET from it to the naphthalenediimide. Then the naphthalenediimide radical anion is pumped (input₂ 1) to transfer its additional electron to the benzenediimide via the naphthalimide. This process happens on the nanosecond timescale. While there is much elegance in this example, we note that only the qualitative aspect of input-output homogeneity is available here. In fact, the quantitative aspect is still not easy to achieve as molecular-scale logic is concerned.

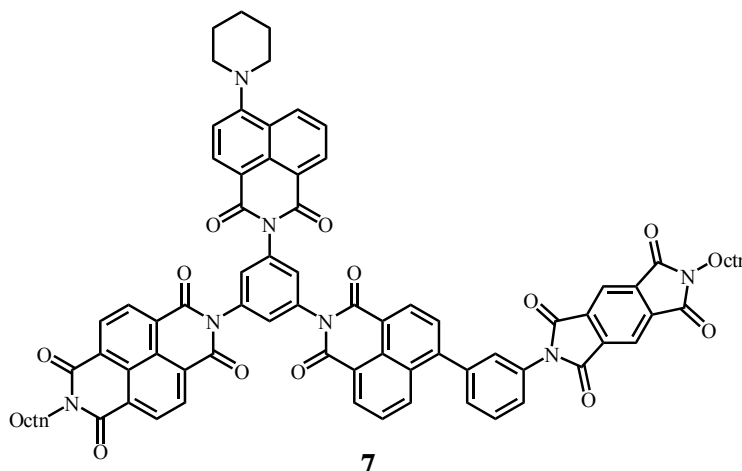


Figure 2.6. Structure of molecular system **7**

XOR Gates

Implementation of the XOR gate in a chemical system is a difficult task. It requires a chemical system that responds to two different stimuli in a complex way. Any of these two stimuli should switch the ion gate, while concomitant presence of both triggering molecules should leave the system in the OFF state.

As a result of the Stoddart and Balzani collaboration, pseudorotaxanes have been persuaded to participate in this type of molecular logic. Threading/unthreading processed of a macrocyclic host (e.g., naphthocrown ether **10**)

and linear guest (e.g., diazapyrenium dication **9**) complex can be influenced by chemical, electrochemical and/or photochemical stimuli with an accompanying recognizable signal [16]. Figure 2.7 shows a molecular XOR gate based on a pseudorotaxane using chemical inputs (acid and base) and a fluorescence output signal from the 2,3-dialkoxy-naphthalene moiety. In the presence of acid or base in the complex threading is not permitted and an output 1 is obtained in the form of emission at 343 nm. In neutral solution (i.e., either no acid or base, or both added simultaneously in stoichiometric amounts) the non-emissive 1:1 complex forms and an output 0 is obtained.

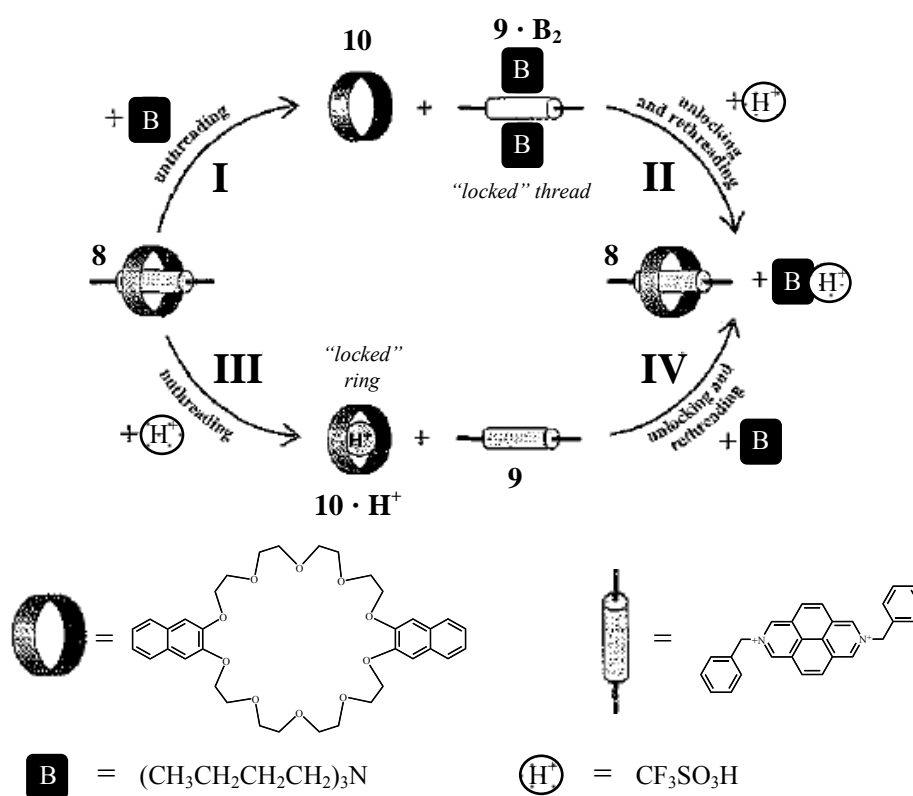


Figure 2.7. Schematic representation of the unthreading/rethreading pattern of pseudorotaxane **8**, which corresponds to an XOR logic function [16]

Balzani and Pina's compound **4** [49] can also be nicely persuaded to show XOR logic behavior when it is combined with $[\text{Co}(\text{CN})_6]^{3-}$. The two inputs are ultraviolet light doses, whereas the output is the optical property of **6**. In the hands

of these authors, some principles from the field of artificial intelligence are also displayed by **4**.

INH Gates

An INHIBIT (INH) logic gate is a result of concatenation of AND and NOT gates, but in contrast to other gates with concatenated NOT, the logic inversion concerns not the output but one of the inputs. Numerous chemically driven INH gates can be based on simple molecular systems and supramolecular assemblies.

The nonfluorescent calix[4]pyrrole-coumarin assembly **11** can bind chloride anions within the calix[4]pyrrole cavity and sodium ions via the carbonyl group. Association with chloride does not change the weak fluorescence. Binding of Na^+ , in turn, increases the fluorescence quantum yield. Concomitant binding of Na^+ and Cl^- results in fluorescence quenching. This behavior is equivalent to the INHIBIT gate with sodium cations and chloride anions inputs and fluorescence output [54].

Fluorescent INH gate is represented by macrocyclic Tb^{III} complexes, **12** [55, 56]. Fluorescence of the Tb^{3+} center can be observed only upon protonation of the quinoline moiety due to efficient electronic energy transfer from the quinoline antenna to the terbium luminophore. However, terbium fluorescence is quenched by molecular oxygen. Therefore, the complex behaves like the INH gate with proton and oxygen inputs and the fluorescence output. Surprisingly, the analogous europium(III) complex does not show this interesting switching pattern.

The only three-input INH molecular gate reported so far is the molecule **13** [19]. It binds calcium via the four armed amino acid receptor, which switches the phosphor to the on state. The phosphorescence of 2-bromonaphthalene is, however, efficiently quenched by molecular oxygen via bimolecular triplet-triplet annihilation. Therefore, phosphorescence is observed only in rigorous absence of oxygen and upon complexation of the fluorophore within the cavity of β -cyclodextrin.

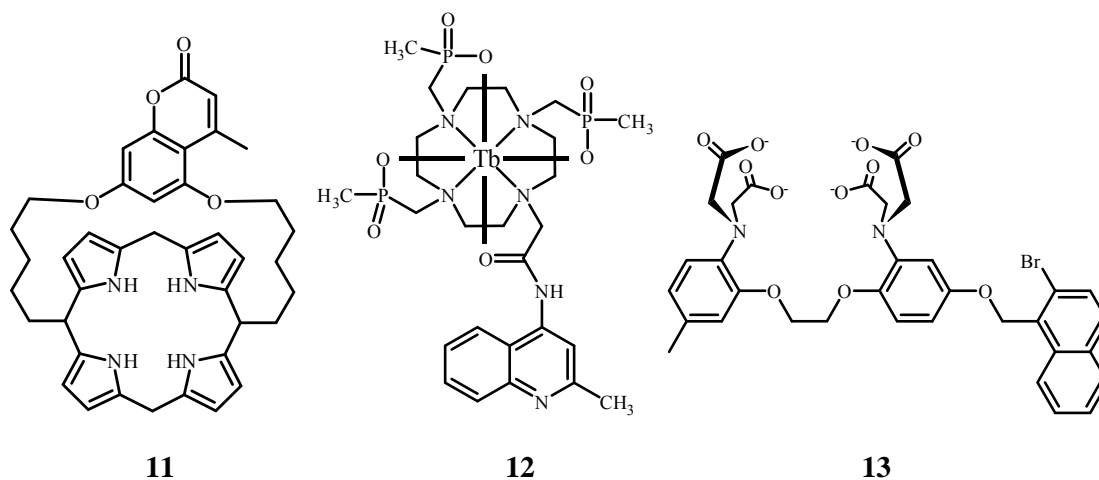


Figure 2.8. Molecular structures of **11**, **12** and **13** which can undergo INH logic operations

Inverted Logic Gates (NOR, NAND, XNOR, and NINH)

Concatenation of NOT gate with other logic gates results in inverted logic gates (NOR, NAND, XNOR, and NINH). There are two main approaches of mimicking these gates in chemical systems: applications of complementary optical outputs (e.g., transmittance instead of absorption) and specific molecular design of the molecular switching element. The first approach corresponds to the switch from positive to negative logic (or vice versa), and some examples were described together with normal logic gates in preceding sections.

NOR logic operations can be obtained from compounds **14** and **15** [19]. Upon ultraviolet irradiation, they fluoresce in the visible spectrum (blue and violet fluorescence, respectively). Protonation or complexation of transition metal cations (Hg^{2+} and Zn^{2+} , respectively) results in the quenching of fluorescence. Therefore, these molecules can be regarded as NOR molecular gates with chemical inputs and optical outputs.

NAND gates have high value in electronics, since multiple copies of these (as well as NOR gates) can be wired up to emulate all the other logic types. There are also several chemical implementations of the NAND functionality. Pyridoimidazolopyrazine derivative **16** is a strong fluorophore [57]. Binding of alkali

or alkaline earth metal cations by the crown ether moiety does not significantly influence the fluorescent properties. Interactions with alkali metal thiocyanates also have no effect on luminescence; electrostatic interactions between thiocyanate and cations are too weak to hold the anion in the proximity of the fluorophore. Calcium and barium cations efficiently bind to the crown moiety and can themselves coordinate thiocyanate, which in turn efficiently quenches the fluorescence in PET process. Supramolecular interactions are also the basis of the **17** NAND gate, reported by Lu and coworkers [25]. The luminescence of the anthryl fluorophore is only slightly sensitive to pH (within pH range of 2 to 8), and in neutral solutions, it is also insensitive to the presence of ATP. Upon protonation, intermolecular interaction becomes much stronger (π - π stacking + electrostatic interaction + hydrogen bonding), which results in significant quenching of the fluorescence due to PET from the adenosyl moiety. Therefore, if protons and ATP are considered as inputs and luminescence intensity as an output, the **17** sensor behaves like the NAND gate.

An example of XNOR logic is a pseudorotaxane consisting of an electron rich tetrathiafulvalene derivative **18** inserted in the cavity of an electron-deficient bipyridinium cyclophane **19** [58]. In CH₃CN, an absorption band associated with the CT interaction is observed at 830 nm. This absorption is taken as the output signal. The two inputs are the positive (+0.5 V) and negative (-0.3 V) potentials sufficient to cause one-electron oxidation and reduction of **18** and **19**, respectively. In both circumstances the complex dissociates and the CT absorption disappears. In summary, electrical stimulation controls the CT absorption (output). A positive logic convention (low = 0, high = 1) was applied to the potential input that controls the redox state of **18**, and a negative logic convention (low = 1, high = 0) was applied to the potential input that governs the redox state of **19**. The resulting truth table corresponds to that of a XNOR gate. It has been remarked [59] that the input string with In₁ and In₂ equal to 1 implies that input potentials +0.5 V and -0.3 V are applied simultaneously to a solution containing the pseudorotaxane compound and not to an individual complex. Of course, the concomitant oxidation of **18** and reduction of **19** in the same pseudorotaxane would be unrealistic. The XNOR operation executed by the

supramolecular system is, therefore, a consequence of bulk properties and not a result of a unimolecular signal transduction.

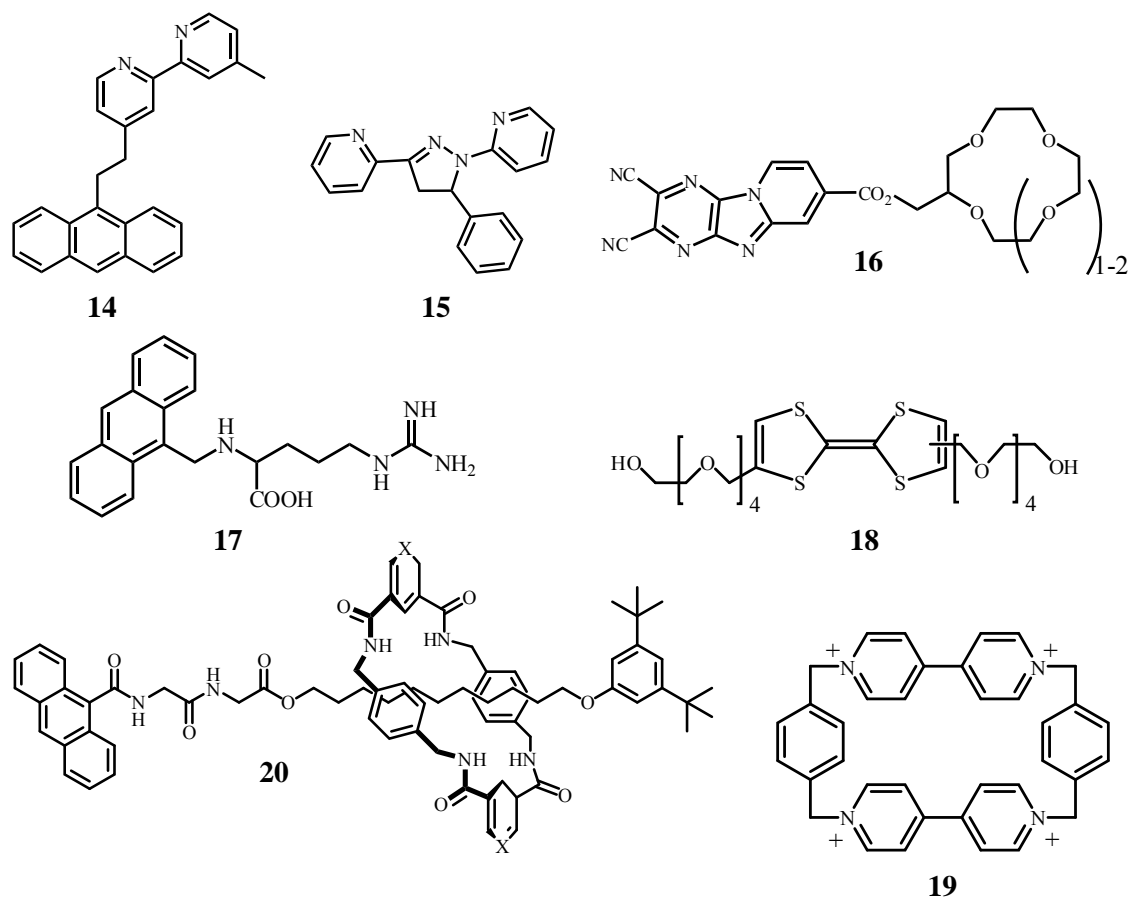


Figure 2.9. Structures of inverted logic gate molecules **14-20**

The supramolecular Non-INHIBIT (NINH) logic gate based on rotaxane **20** was recently reported [60]. The switching system is composed of a thread equipped with anthryl and di-*t*-butylphenyl stoppers and two solvophobic stations, glycil-glycine and the C₁₁ alkyl chain. The amide macrocycle contains pyridine moieties that can quench the luminescence of the anthracene moiety. In nonpolar media, the macrocycle forms hydrogen bonds with the glycil-glycine chain and resides close to the anthracene terminal. In strongly polar solvents (formamide and DMSO), the macrocycle moves toward the alkyl chain, and quenching becomes negligible. Protonation of the pyridine moieties switches on the anthracene

fluorescence irrespective of the solvent polarity. This behavior can thus be described as the NINH Boolean function.

Reconfigurable and Superimposed Molecular Logic Devices

Reconfigurable logic devices are very important components of modern electronic devices. They usually are large arrays of logic gates, and the internal connections between particular elements can be changed on demand. Therefore, these electronic systems are very flexible and can be programmed (or configured) to fulfill numerous tasks.

Superimposed logic devices are unprecedented devices found only in molecular systems. Their operation mode depends on the way information is read from the device, e.g., using different analytical wavelengths. They are conceptually somehow related to quantum logic gates, where the output state is a superposition of all possible output states.

Another reconfigurable logic device is based on the anthracene fluorophore with a long polyamine tail **21** [61]. Fluorescence of this molecule is efficiently quenched by PET from the polyamine chain. Protonation or coordination of Zn^{2+} or Cd^{2+} cations inhibits the photoinduced electron transfer even at high pH and switches on the fluorescence. Coordination of some other cations (Cu^{2+} and Ni^{2+}) results in fluorescence quenching of the partially protonated compound. Due to the diversity of responses of various chemical stimuli, this system should be regarded as a reconfigurable logic device with fluorescence output. Application of Zn^{2+} and Cd^{2+} as inputs yields an OR gate, while when the inputs are Ni^{2+} and Cu^{2+} , the anthracene derivative behaves as the NOR gate. Another logic operation can be performed when one input taken from the first group and the other from the second one (e.g., Zn^{2+} and Cu^{2+}). In this case, fluorescence can be observed only in the presence of Zn^{2+} and the absence of Cu^{2+} , which corresponds to INH operation.

The next superimposed logic system is based on the benzothiazole derivative **22** [62]. Solutions of **22** are yellow (λ_{max} 413 nm) and only weakly fluorescent (~ 500 nm, $\Phi = 0.05$). Interactions between the azacrown ether moiety and calcium ions result in a slight hypsochromic shift of the absorption band and a

decrease of fluorescence intensity. The thiazacrown moiety can, in turn, interact with Ag^+ cations. This reaction also induces a small hypsochromic shift of the absorption band and also a strong increase of the fluorescence quantum yield ($\Phi = 0.27$). In the presence of both Ca^{2+} and Ag^+ results in a strong hypsochromic shift of the absorption band and fluorescence quenching. If fluorescence at 500 nm and absorbance at 440 nm are taken as two outputs, they yield the NAND and INH responses, respectively.

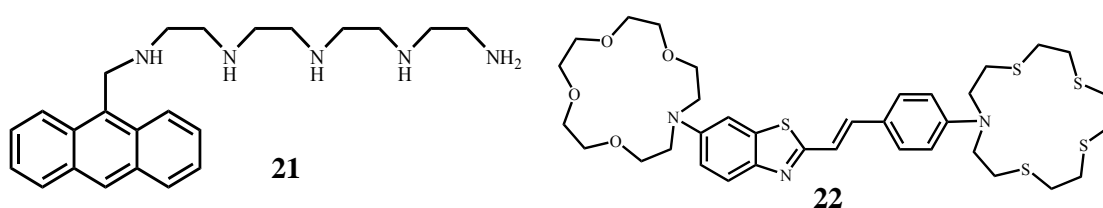


Figure 2.10. Structures of reconfigurable and superimposed molecular logic devices **21** and **22**

2.3 Optodes

The ion selective optode is one of the optical chemical sensors (so-called optodes or optrodes) which have attracted chemist's interest since the 1970s. The essence of the usefulness of the ion selective optode is the „ion selectivity“ associated with the highly selective complexation of an ionophore (either neutral or charged) with an analyte ion in optical chemical sensing. Among many complexing agents used so far, electrically neutral and lipophilic ionophores, which are the selective compounds in the widely used ion selective electrodes (ISEs), attract most interest. In optode membranes, they have been found to exhibit the same excellent and analytically relevant selectivity for many ions as in electrode membranes.

A typical ion selective optode contains an ionophore L, which selectively forms a complex with a primary metal ion I^{z+} and a chromoionophore C, a lipophilic dye, that interacts with a reference ion (H^+) and changes optical properties upon protonation. The third additive is a lipophilic cation-exchanger. Because the concentration of the ion-exchanger in the matrix is limited, the competition between two ions (primary ion and H^+) for the ion-exchange sites affects the fraction of protonated chromoionophore CH^+ and determines the sensor response.

It is important to distinguish between two different types of sensing layers for charged species to understand how these sensors function. [63]

1) *Optodes based on surface phenomena.* The active components are immobilized near the interface or on the surface of the optical element or porous matrix, so that the active site is located in the sample solution. Very often, the recognition molecule is immobilized, either by a covalent binding, or by its physical adsorption on the surface (Figure 2.11). Errors in the determination of the sample's pH are mainly associated with a change in ionic strength of the sample. It influences both the activity coefficient of the charged form of the indicator and the surface potential, which is responsible for the relationship between the measured pH at the surface and the pH of the bulk.

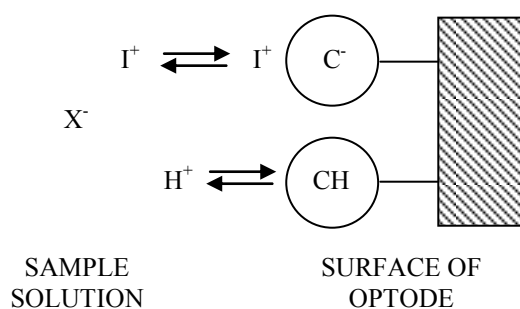


Figure 2.11. Schematic representation of a pH optode based on an anionic indicator dye directly immobilized on the surface of the optical element.

2) *Bulk optodes.* The active components are uniformly entrapped in the bulk of a homogeneous sensing layer. Such optodes are based on a mass transfer of the ions from the sample into the bulk of the sensing layer to get an adequate optical signal. Since the electroneutrality is conserved on the sensing layer, these optodes respond to products (extraction system) or to ratios (ion-exchange system) of the ion activities.

All optode membranes discussed here are considered as single phase and thus, in the thermodynamic sense, as a region of space that has uniform properties throughout.

2.3.1 Response Mechanism [33]

Optical Sensors for Ionic Analytes. While hydrophobic polymeric films containing neutral ionophores and lipophilic ionic sites are a well-suited matrix for ion-selective electrode membranes, the realization of optical sensors that exhibit similar selectivity and sensitivity as their ISE counterparts requires somewhat different considerations. An optical signal change must usually be induced by a concentration change of a component inside a thin polymeric film. Since ion-selective electrode membranes are ideally permselective ion exchangers, the concentrations of ionophore and its complex in the organic phase are practically constant as long as a Nernstian behavior of the electrode is observed. A signal change of a corresponding bulk optode film (i.e., one that has the same composition as the ISE membrane) is expected outside the Nernstian response range of the electrode. Since electroneutrality must hold for the bulk phase, bulk optodes based on hydrophobic films cannot be sensitive to one ion alone. Instead, well-defined phase transfer equilibrium of two distinct ions has to be established. This process is shown schematically in Figure 2.12 for neutral ionophores. Depending on the charge signs of the two involved ions, either a competitive ion exchange or carrier-mediated coextraction equilibrium is responsible for the optode response. Preferably, a complexation reaction of at least one of the two ions should lead to an optical response, e.g. due to changes in absorbance, fluorescence, phosphorescence, or reflective index. Most reports on bulk optode films have made use of the selective interaction of hydrogen ions with lipophilized or immobilized pH indicators as chromoionophores. This has obvious advantages, since the sample pH can be varied and buffered over a wide range and lipophilized pH indicators with a large variety of different basicities are now available. In addition, neutral H^+ -ionophores belong to the most selective ones and the complexation of these compounds with other cations can usually be neglected.

FOR CATIONIC ANALYTES

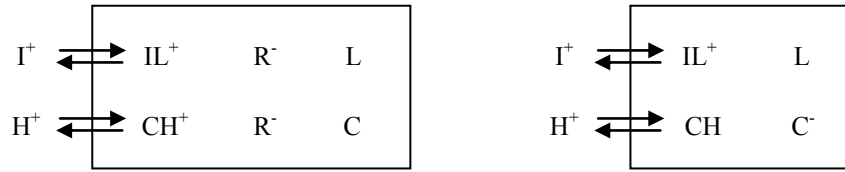


Figure 2.12. Neutral-carrier-based optodes with neutral or charged chromoionophores (L, neutral carrier; C and C⁻, neutral and charged H⁺-chromoionophores; R⁻ negatively charged ionic sites). Squares indicate species in the organic phase.

Here, we will focus on the theory of the ion-exchange mechanism that has been described most often for polymeric films containing a neutral ionophore L forming complexes IL_n^{z+} with the cationic analyte I^{z+} , a neutral chromoionophore C that binds H^+ to form CH^+ , and lipophilic anionic additives R^- . Other systems can often be described by complete analogy. The overall ion-exchange equilibrium between sample and organic film is written as [64]



with the corresponding exchange constant

$$K_{exch}^{IL_n} = \left(\frac{a_H[C]}{[CH^+]} \right)^z \frac{IL_n^{z+}}{a_I[L]^n} = \left(\frac{K_a}{k_H} \right)^z k_I \beta_{IL_n} \quad (2)$$

which is a function of the relative lipophilicities k_I and k_H of I^{z+} and H^+ respectively, the stability constant β_{IL_n} for the ion-ionophore complex, and the acidity constant K_a for the chromoionophore. The latter two are defined for the organic phase. It is assumed that concentrations within the organic phase are proportional to activities. This assumption considerably simplifies the mass and charge balances used for eq 2. Subsequently, eq. 2 is combined with the electroneutrality condition

($R_T^- = [CH^+] + z[IL_n^{z+}]$) and mass balances for the ionophore ($L_T = [L] + n[IL_n^{z+}]$) and chromoionophore ($C_T = [C] + [CH^+]$) in the polymeric film, giving the optode response function as

$$a_I = (zK_{exch}^{ILn})^{-1} \left(\frac{\alpha}{1-\alpha} a_H \right)^z \times \frac{R_T^- - (1-\alpha)C_T}{\{L_T - (R_T^- - (1-\alpha)C_T)(n/z)\}^n} \quad (3)$$

where the normalized absorbance α is the relative portion of the unprotonated form of the chromoionophore ($\alpha = [C]/C_T$). Since the optode film is in chemical equilibrium with the sample solution, the ratio of free sample ion activities (a_I/a_H^z), not of concentrations, is measured. Equation 3 describes an implicit sigmoidal response function that cannot generally be solved for α . The measured absorbance A at a given equilibrium can be related to α by measuring the absorbances of the fully protonated (A_P) and nonprotonated form (A_D) of the chromoionophore

$$\alpha = \frac{A_P - A}{A_P - A_D} \quad (4)$$

It is evident from eq 3 that the equilibrium not only depends on the analyte ion concentration but also on the pH value, i.e., the pH has to be kept constant or determined independently for accurate analyte ion activity measurements. Another consequence of eq. 3 is the fact that the ion-exchange equilibrium can be shifted to lower or higher activity ranges by choosing a system with a different exchange constant, i.e., by changing either the ionophore or chromoionophore with one that forms a complex with a different stability. An additional important feature of such an optode response function is the dependence on the charge of the extracted cation and the stoichiometry of the complex. The latter information cannot be obtained from measurements within the Nernstian response range of corresponding ion-selective electrodes.

Bulk optodes have gained considerably in practical reliability, and can be considered as inexpensive alternatives to certain conventional analytical methods.

By changing the membrane composition, an appropriate adjustment of the parameters to a specific set of requirements is possible. For each application, the optimization of all optode characteristics should be addressed, rather than a single property, owing to the interdependence of most parameters.

Very low detection limits, high sensitivities and attractive sensor designs are the outstanding advantages of such optodes. In contrast to potentiometric sensors, they allow the direct detection of neutral species in different phases. Unfortunately, most optodes still suffer from limited lifetime, which should be alleviated by the use of more lipophilic membrane components or immobilization procedures. An improved lifetime which is not achieved at the expense of response time is highly desirable. [65]

2.3.2 The Utilization of Bulk Optodes

Ion selective bulk optodes have been developed in a few decades. Among them, optodes based on ionophores and chromoionophores were used to successfully measure several clinically important ion species such as lithium, sodium, potassium, ammonium, calcium and chloride. [66-73, 28, 29] Improving of the detection limit and tuning the dynamic range to the desired region of interest are needed for further applications. In recent years, miniaturized forms of the bulk optode sensors have emerged, and microtiter plate based optodes, microbeads and nanospheres have been successfully developed by surface coating, polymerization, sonication, or by a particle caster based on microfluidics. [74-78] Smaller amounts of sample and shorter measurement times are required for such sensors. Besides blood electrolytes, such sensors are also promising for environmental trace analysis such as lead and silver, with subnanomolar detection limits and short response times. [32]

Bulk optode systems consist of components that can exist in 2 different states (protonated/deprotonated form of chromoionophores) and the appearance of primary ion or proton is a chemical stimuli capable of switching the system from one state to the other reversibly. These systems may be regarded as molecular logic systems.

In this study, we employed a sodium and potassium/hydrogen ion selective optode in „proof-of-concept” experiments for another molecular logic gates.

CHAPTER III

EXPERIMENTAL

3.1 Apparatus

A Cary[®] 50 UV-Vis spectrophotometer (Varian) was used to record all spectra and absorbance measurements. A homemade holder was used to hold a membrane plate. All pH values were determined with an Orion 2-Star Benchtop pH meter (Thermo Fisher Scientific).

3.2 Chemicals

All chemicals used for membrane preparation were purchased in selectophore or puriss quality form suppliers listed in Table 3.1.

Table 3.1. Chemicals list

Chemicals	Supplier
<i>p-tert</i> -Butylcalix[4]arene-tetraacetic acid tetraethyl ester (Na(X))	Fluka
Potassium ionophore I (Valinomycin)	Fluka
Potassium tetrakis[4-chlorophenyl] borate, KTpCIPB	Fluka
Bis(2-ethylhexyl)sebacate, DOS	Fluka
High molecular weight poly(vinyl chloride), PVC	Fluka
9-(Diethylamino)-5-octadecanoylimino-5H-benzo[a]phenoxazine (Chromoionophore I, ETH 5294)	Fluka
9-(Diethylamino)-5-[4-(15-butyl-1,13-dioxo-2,14-dioxanodecyl)phenyl- imino]benzo[a]phenoxazine (Chromoionophore VII, ETH 5418)	Fluka
9-[4-Diethylamino-2-(octadecanoyloxy)styryl]acridine (Chromoionophore XIV)	Fluka
Stabilizer-free tetrahydrofuran (THF)	Fluka
Magnesium acetate tetrahydrate, Mg(CH ₃ COO) ₂ ·4H ₂ O	Fluka
Tris (hydroxymethyl)-aminomethane, C ₄ H ₁₁ NO ₃	Carlo Erba
Sodium Nitrate, NaNO ₃	Carlo Erba
Potassium nitrate, KNO ₃	BDH

Nile Blue-urea was prepared according to previously published procedures. [79] All solutions were prepared with Milli-Q (Bedford, MA, USA) water using Nanopure Millipore water purification system. Structures of components of sodium and potassium selective optodes are shown in Figure 3.1.

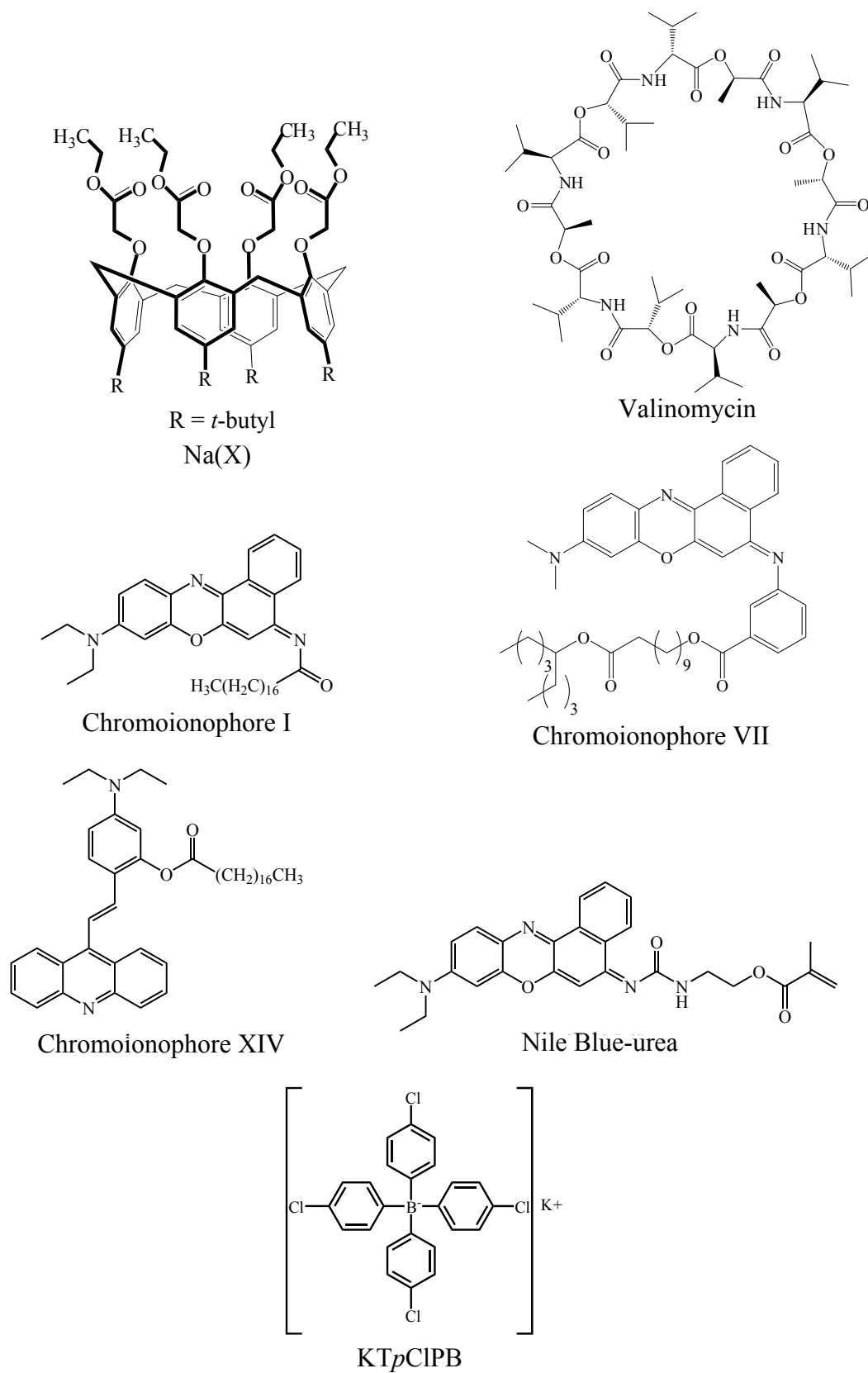


Figure 3.1. Major components of sodium/potassium selective optodes

3.3 Membrane Preparation

Generally, an optode cocktail (90 mg total mass) consisted of poly(vinyl chloride) and the plasticizer DOS (1:2 by mass) in addition to the following components; for sodium and potassium optodes, 10 mmol kg⁻¹ of either sodium ionophore (Na(X)) or valinomycin, 5 mmol kg⁻¹ of KTpCIPB as ion exchanger, 2.5 mmol kg⁻¹ of chromoionophore (either ETH 5294, ETH 5418, chromoionophore XIV or Nile Blue-urea); for mixed ionophore optodes, 5 mmol kg⁻¹ of Na(X) and Valinomycin, 5 mmol kg⁻¹ KTpCIPB, 2.5 mmol kg⁻¹ of chromoionophore (either chromoionophore XIV or Nile Blue-urea). Optode thin films were prepared by dissolving the mixture in 2 mL THF. The optode films were casted by pipetting 50 μ L of cocktail onto 22-mm (No.1) square cover glass slides. The freshly prepared films were dried in air for at least 30 min prior to use.

The concentration of each optode components are shown in Table 3.2. A typical membrane composition for the optode membrane is kept in the order of C < R⁻ < L. [33]

Table 3.2. The amount of components in optodes

Components	mmol kg ⁻¹	mg
<i>Sodium selective optode</i>		
Na(X)	10	0.89
KTpCIPB	5	0.22
Chromoionophore	2.5	
- Chromoionophore I		0.13
- Chromoionophore VII		0.16
- Chromoionophore XIV		0.14
- Nile Blue-urea		0.11
<i>Potassium selective optode</i>		
Valinomycin	10	1.00
<i>Mixed ionophore optode</i>		
Na(X)	5	0.45
Valinomycin	5	0.50

3.4 Logic Gate Preparation

The prepared membranes were placed in a buffer solution of pH 4.0 for 15 min to reach equilibrium. Then the sensing membrane was put in a sample containing an appropriate concentration of sodium and/or potassium ions for another 15 min to reach equilibrium. The absorbance value of the system was measured over the wavelength range of 400-750 nm. A glass slide without membrane was used as blank for absorbance measurement. Measurements were performed in a batch mode. The analytical performance of potassium- and sodium-selective optodes can be evaluated by soaking the membranes in standard solutions containing the respective primary ion from 1.0×10^{-4} to 1.0×10^{-1} M in 0.001 M Acetate-Acetic (pH 3-6) or Tris-HCl (pH 7-10) buffer.

Two ions (H^+ , Na^+ or K^+) were chosen to be inputs of an experiment, and an output would be an absorbance at λ_{max} of protonated or unprotonated forms of the chromoionophore. For conventional optodes, logic value 0 of the input A was a high pH (H^+ concentration) while logic value 1 was a low pH. For input B, logic value 0 was a buffer solution at the pH when the input A was 0, and logic value 1 was either $NaNO_3$ or KNO_3 (1.0×10^{-4} , 1.0×10^{-3} , 1.0×10^{-2} or 1.0×10^{-1} M) in a buffer solution at the pH when the input A was 1. For mixed ionophore optodes, input A and input B were sodium ion and potassium ion, respectively. The absence of the metal ion was considered as logic value 0, and the presence of 1.0×10^{-1} M $NaNO_3$ and/or 1.0×10^{-1} M KNO_3 was considered as logic value 1 in a buffered solution of a desired pH.

3.5 Threshold Value for Absorbance Output

Protonated absorbance and nonprotonated absorbance are absorption that each specifies a degree of protonation in the optode system. The value chosen for 1 or 0 represents the difference between the corresponding spectra. Threshold values are determined by fix degree of deprotonation (α) at 0.6. The measured absorbance A at a given equilibrium can be related to α by measuring the absorbances of the fully protonated (A_P) and nonprotonated form (A_D) of the chromoionophore:

$\alpha = (A_P - A) / (A_P - A_D)$. Details of calculations are provided in Appendix D.

CHAPTER IV

RESULTS AND DISCUSSION

4.1 Matched ionophore-primary ion

The optode system was operated by 2 variable factors which were used as chemical inputs of optode logic gates, proton (input A) and sodium or potassium ion (input B). The output of the optode (the spectral change of a chromoionophore) was read out in terms of the absorbance at appropriate wavelengths. Theory of ion-exchange mechanism was described most often for a polymeric film containing a neutral ionophore L forming complexes IL_n^{z+} with the cationic primary ion I^{z+} , a neutral chromoionophore C that bound to H^+ to protonated form CH^+ , and lipophilic anionic additives R^- . A competitive ion exchange equilibrium is responsible for the optode response. The overall equilibrium between a sample and an organic film can be written as equation (4.1). [64]



Sodium and potassium selective optode were studied. The equilibrium of the studied optode could be written as



The eq. (4.2) and (4.3) represent the ion exchange equilibrium between solution and the membrane phase. It can be seen that the degree of protonation of the chromoionophore is respect to the competition between H^+ and Na^+/K^+ in the solution phase. Therefore, the degree of protonation decreased with the increasing of metal ion concentration. This mechanism causes the color of the membrane changed depending on the ratio of the C/CH^+ form of the chromoionophore.

Phase transfer equilibria of sodium/potassium and hydrogen ions are shown schematically in Figure 4.1.

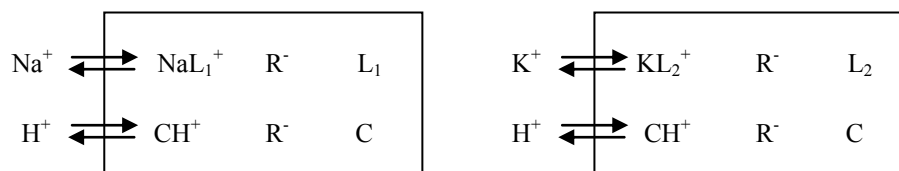


Figure 4.1. Phase transfer equilibria of neutral-carrier-based optode (L_1 , tetramethoxyethylene calix[4]arene, L_2 , valinomycin; C, neutral H^+ -chromoionophores; R^- negatively charged ionic sites). Squares indicate species in the organic phase.

The optode logic gates would depend on the equilibrium between 2 inputs, Na^+ (or K^+) and H^+ , which normally gave rise to INHIBIT (INH) and Non-INHIBIT (NINH) logic gates. For the membrane containing chromoionophore I, the absorbance intensity at 540 and 665 nm was encoded as the outputs (O1 and O2, respectively). The absorbances at 530 and 670, 435 and 660, 540 and 665 nm were the outputs O1 and O2 of chromoionophore VII, Chromoionophore XIV and NB-urea, respectively. Table 4.1 showed wavelength assigned to be output O1 and output O2 for each chromoionophore. Output O1 and O2 represent deprotonated and protonated λ_{max} wavelength of chromoionophore, respectively, as shown in Figure 4.2.

Table 4.1. Wavelengths for outputs O1 and O2 of various chromoionophores

Chromoionophore	Wavelength for output O1 absorbance (nm)	Wavelength for output O2 absorbance (nm)
Chromoionophore I	540	665
Chromoionophore VII	530	670
Chromoionophore XIV	435	660
Nile Blue-urea	540	665

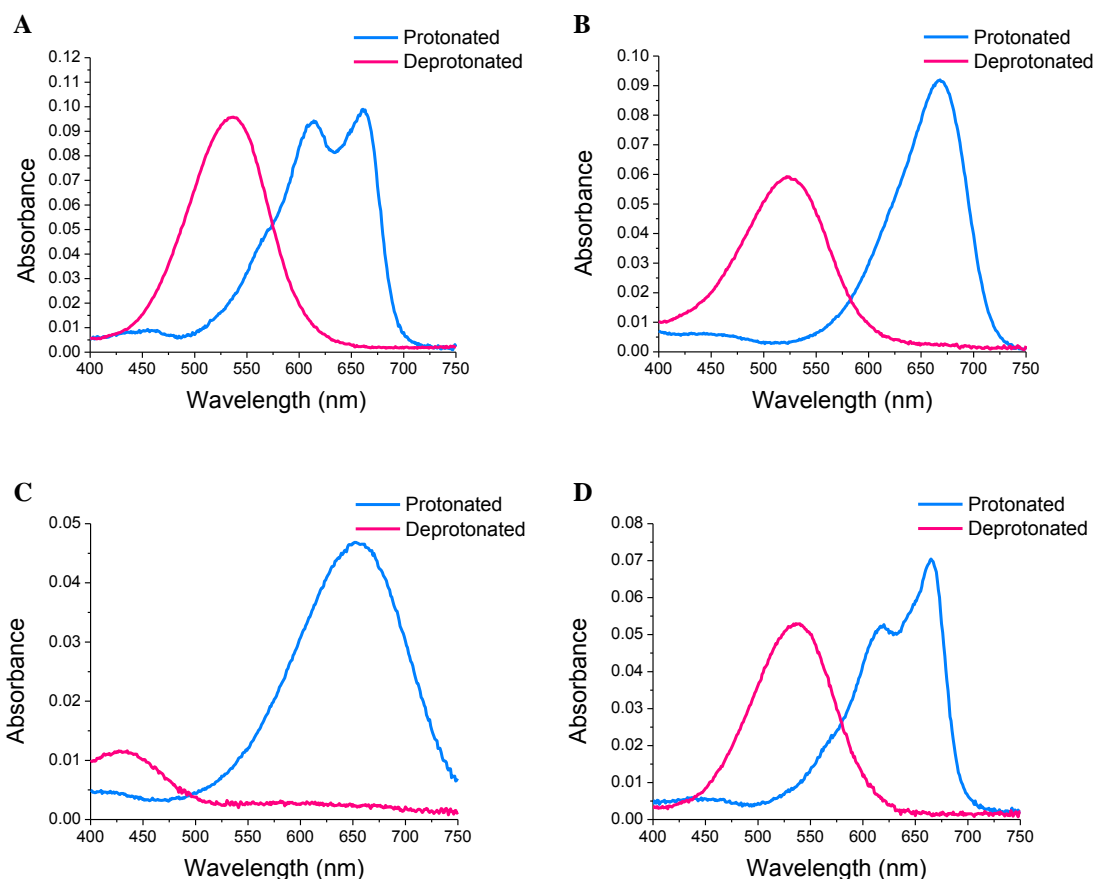
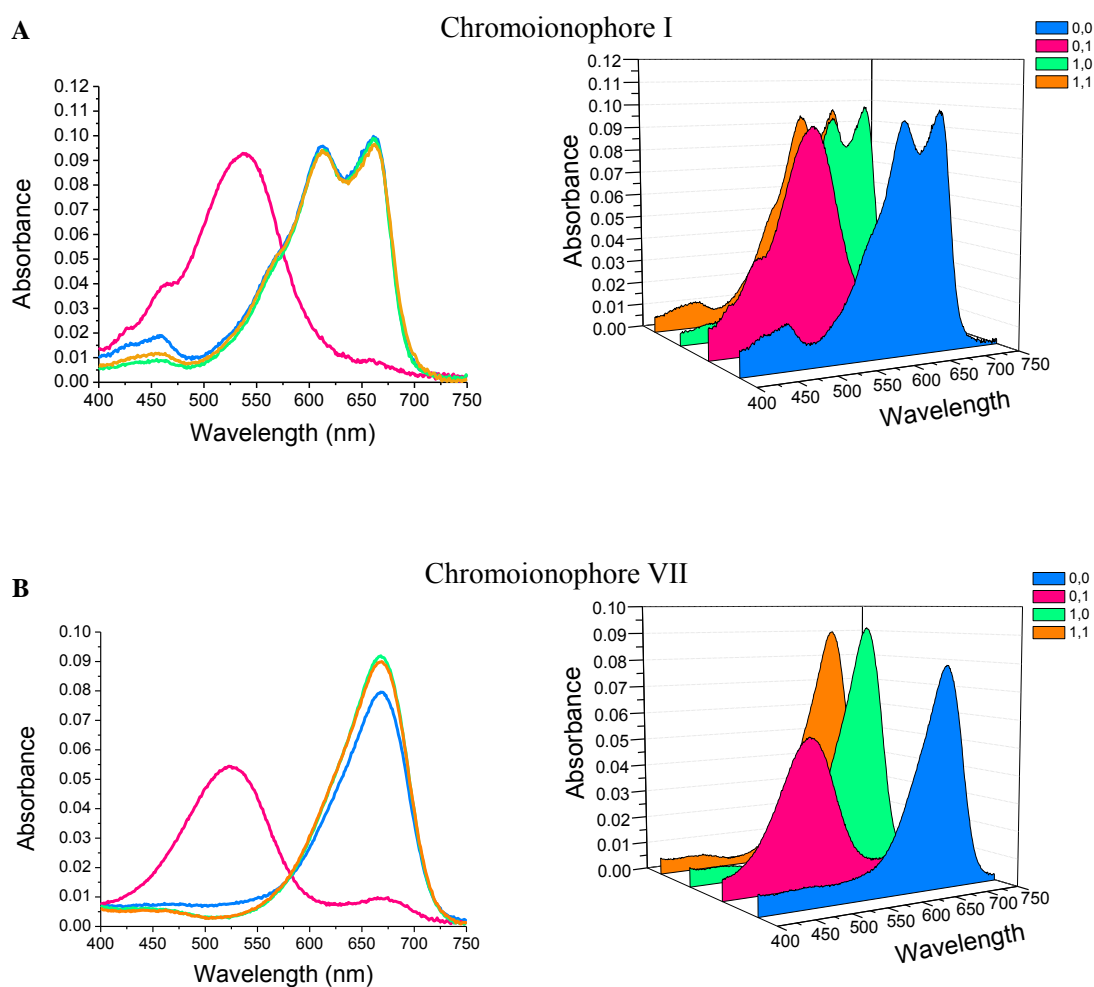


Figure 4.2. Absorbance features of protonated and deprotonated wavelength (O1 and O2) using studied chromoionophore: (A) Chromoionophore I, (B) Chromoionophore VII, (C) Chromoionophore XIV, (D) Nile Blue-urea.

We used sodium ionophore-sodium ion optodes system as a representative for an explanation. All chromoionophores produced INH A logic gate for output O1 and NINH A gate for output O2 at a pH lower than a pK_a of a chromoionophore. Absorbance variations of all chromoionophores were shown in Figure 4.2, and the truth table was shown in Table 4.2. The INH A gate gave an output 1 only if the input A was in configuration 0, while input B was in configuration 1. This INH A gate required the addition of the medium concentration of Na^+ in the low concentration of H^+ . Figures 4.3A and 4.3D showed a strong absorbance at 540 nm (output O1) for the combination 0,1 of chromoionophore I and Nile Blue-urea optodes, also, Figure 4.3B and 4.3C showed logic value 1 of O1 for chromoionophore VII and XIV respectively. If both inputs were FALSE, configuration (0,0), this condition would occurred at the

low concentration of H^+ , and there was no Na^+ in the solution. In the low pH buffer solution, configuration (1,0), also did not lead to the absorption band of the deprotonated state. When inputs were in configuration (1,1), the competitive extraction between H^+ and Na^+ into organic membrane occurred. These 3 configurations caused no significant variation in the absorbance at 540 nm. As a counterpart of the deprotonated λ_{max} of chromoionophore (O1), the absorbance of output O2, protonated λ_{max} of chromoionophore I and Nile Blue-urea, at 665 nm gave NINH A logic gates.



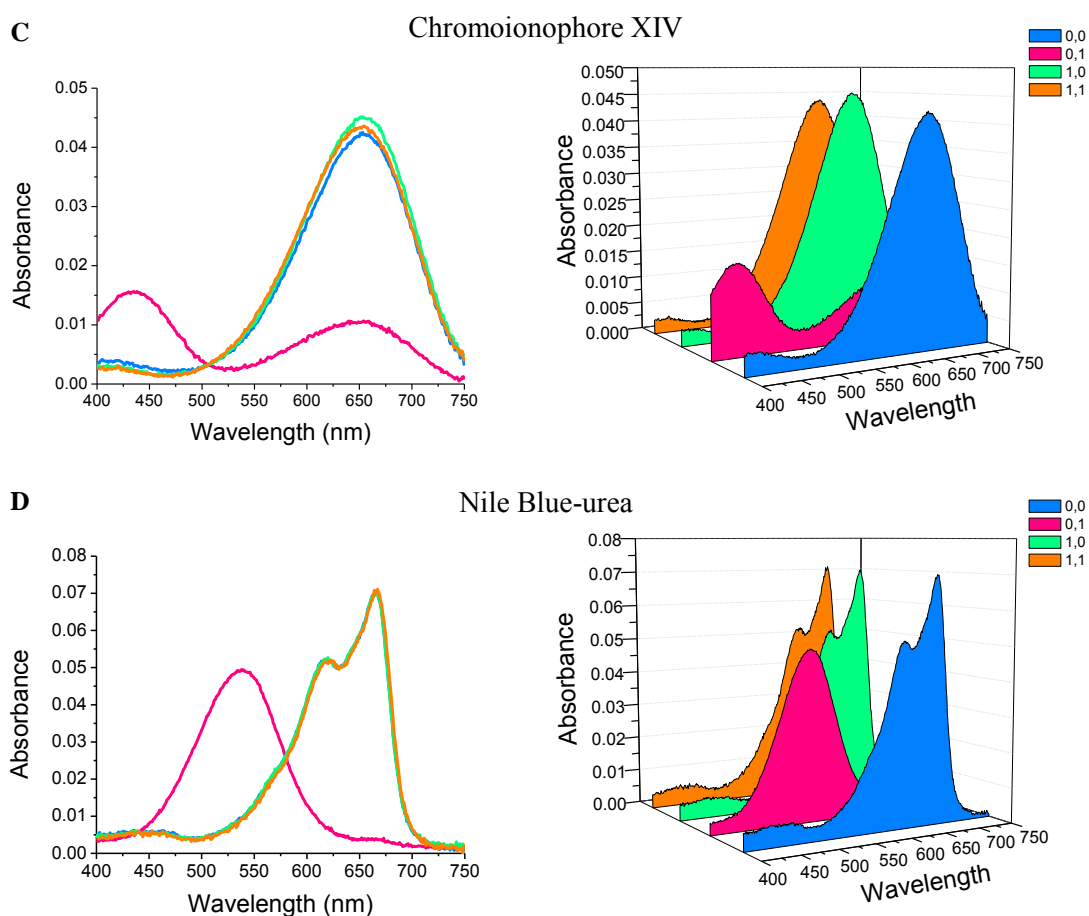


Figure 4.3. Absorbance features of the INH A and NINH A gates of sodium optode using studied chromoionophores: (A) Chromoionophore I (1.0×10^{-1} M NaNO_3 pH 3, pH 7) (B) Chromoionophore VII (1.0×10^{-2} M NaNO_3 pH 3, pH 6) (C) Chromoionophore XIV (1.0×10^{-3} M NaNO_3 pH 3, pH 5) (D) Nile Blue-urea (1.0×10^{-1} M NaNO_3 pH 3, pH 7) Input combination 0,0: blue; 0,1: pink; 1,0: green and 1,1: orange.

Table 4.2. Truth table corresponding to INH/NINH A and B gates

Input		Output			
A	B	INH A	NINH A	INH B	NINH B
0	0	0	1	0	1
0	1	1	0	0	1
1	0	0	1	1	0
1	1	0	1	0	1

A = H^+ and B = Na^+ or K^+

The INHIBIT B gate was basically the equivalent of the INHIBIT A gate, except for the fact that the output 1 was obtained when the input A was 1 and the input B was 0. To obtain this gate, the solution pH should be low and no complexation occurred. Chromoionophore VII and Chromoionophore XIV possessed pK_a 8.6 [80] and 5.5 [81], respectively. The membrane containing these chromoionophores could produce INH/NINH B logic gates at pH higher than 4.0. New logic gates were not found in the systems of Chromoionophore I and Nile Blue-urea that have higher pK_a (11.4 [80] and 9.8 [79]). Figures 4.4A and 4.4B showed strong absorbances at 670 and 660 nm (output O2) for the combination (1,0) of chromoionophore VII and XIV optodes. The counterpart of INH B was also found in the output O1 in the same manner as INH/NINH A logic gates. The value chosen for 1 or 0, threshold values, are determined by fix degree of deprotonation (α) at 0.6. The calculated threshold values for each gate were shown in Figure 4.5.

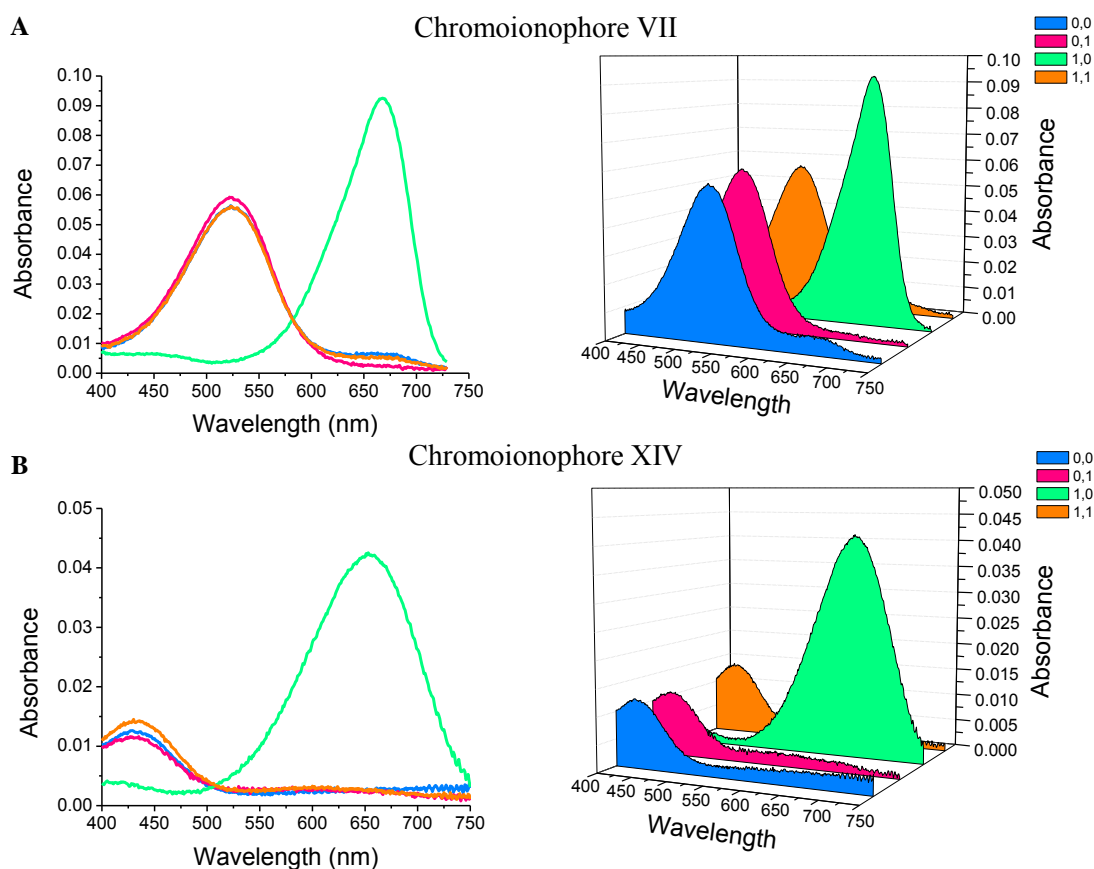


Figure 4.4. Absorbance features of the INH B and NINH B gates of sodium optode using studied chromoionophores: (A) Chromoionophore VII (1.0×10^{-1} M NaNO_3 pH

5, pH 10) (B) Chromoionophore XIV (1.0×10^{-1} M NaNO₃ pH 5, pH 10) Input combination 0,0: blue; 0,1: pink; 1,0: green and 1,1: orange.

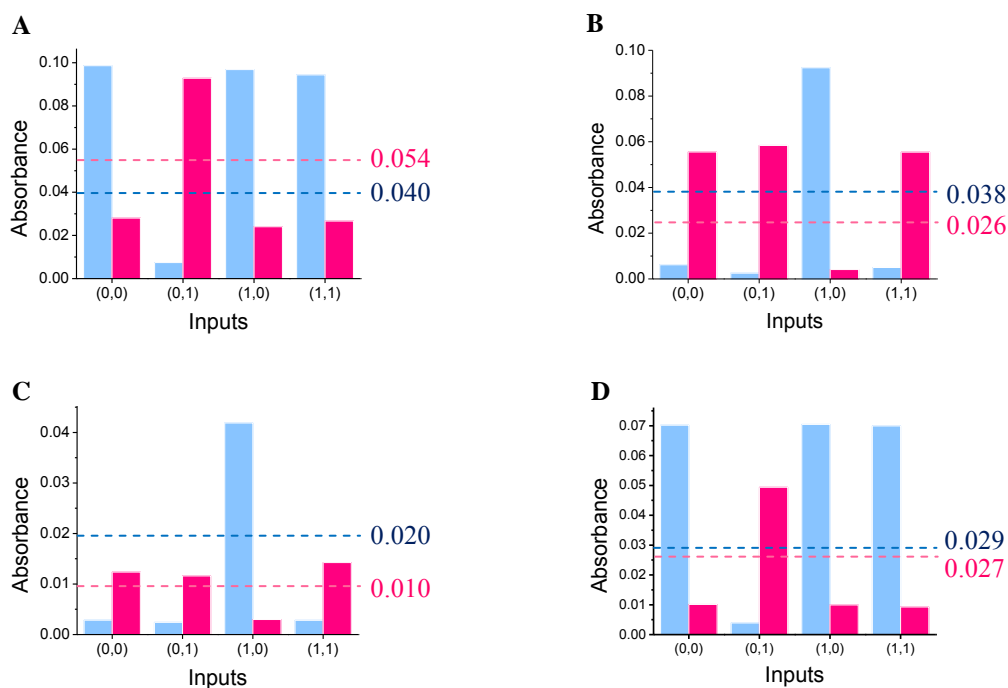


Figure 4.5. Bar diagram featuring the logic operation of the optical systems: (A) Chromoionophore I (B) Chromoionophore VII (C) Chromoionophore XIV (D) Nile Blue-urea Dash line shows values separating digital 0 and 1 output signals produced by the systems. Pink bar referred to output O1 signal, blue bar refers to output O2 signal.

Conditions for the sodium bulk optode to obtain INH A/NINH A and INH B/NINH B gates for various chromoionophores were collected in Table 4.3.

Valinomycin was known to complex well with K⁺ ion. Potassium selective bulk optode showed similar results to sodium selective bulk optode due to the same response mechanism of the optode membrane. Potassium optode also operated INH/NINH A and B but not as many conditions as the sodium optode as shown in Table 4.4 because the amino acid in valinomycin ring gave some contribution to pH of the membrane. The absorption bands were shown in Figure 4.6. These gates may be found in all other ion selective optodes as a result of a similar response mechanism.

Table 4.3. pHs and metal concentrations which operated INH, NINH, AND, NAND, OR and NOR logic gates for sodium optodes.

pH ^a	INH/NINH A and AND/NAND ^b				INH/NINH B and OR/NOR ^b			
	Concentration of Na ⁺ (M)				Concentration of Na ⁺ (M)			
1,0	10 ⁻¹	10 ⁻²	10 ⁻³	10 ⁻⁴	10 ⁻¹	10 ⁻²	10 ⁻³	10 ⁻⁴
3,5		BC	BC					
3,6	AD	BD	BC	C				
3,7	AD	AD	D					
3,8	ACD	AD	AD	D				
3,9	AD	AD	AD	D				
3,10	D	D	D	D	C			
4,6	AD	D	BC	C				
4,7	AD	AD	D					
4,8	AD	AD	AD	D	BC	C		
4,9	AD	AD	AD	D	BC	C		
4,10	D	D	D	D	BC	C		
5,7		D	D					
5,8		AD	AD	D	BC	BC	BC	
5,9		AD	AD	D	BC	BC	BC	
5,10		D	D	D	BC	BC	BC	
6,8		A	AD	D	BC	BC	BC	C
6,9		A	AD	D	BC	BC	BC	C
6,10				D	BC	BC	BC	C
7,9			A	AD				
7,10				D				

^a Input values of pH were alternated in the case of AND/NAND and OR/NOR gates.

^b A, B, C and D referred to chromoionophore I, VII, XIV and NB-urea, respectively.

Table 4.4. pHs and metal concentrations which operated INH, NINH, AND, NAND, OR and NOR logic gates for potassium optodes.

pH ^a	INH/NINH A and AND/NAND ^b				INH/NINH B and OR/NOR ^b			
	Concentration of K ⁺ (M)				Concentration of K ⁺ (M)			
1,0	10 ⁻¹	10 ⁻²	10 ⁻³	10 ⁻⁴	10 ⁻¹	10 ⁻²	10 ⁻³	10 ⁻⁴
3,5					C	C	C	
3,6					BC	BC	BC	
3,7					BC	BC	BC	
4,6		A	A		BC	BC	BC	C
4,7		A	A	A	BC	BC	BC	C
5,7				A	C	C	C	

^a Input values of pH are alternated in the case of AND/NAND and OR/NOR gates.

^b A, B and C referred to chromoionophore I, VII and XIV, respectively.

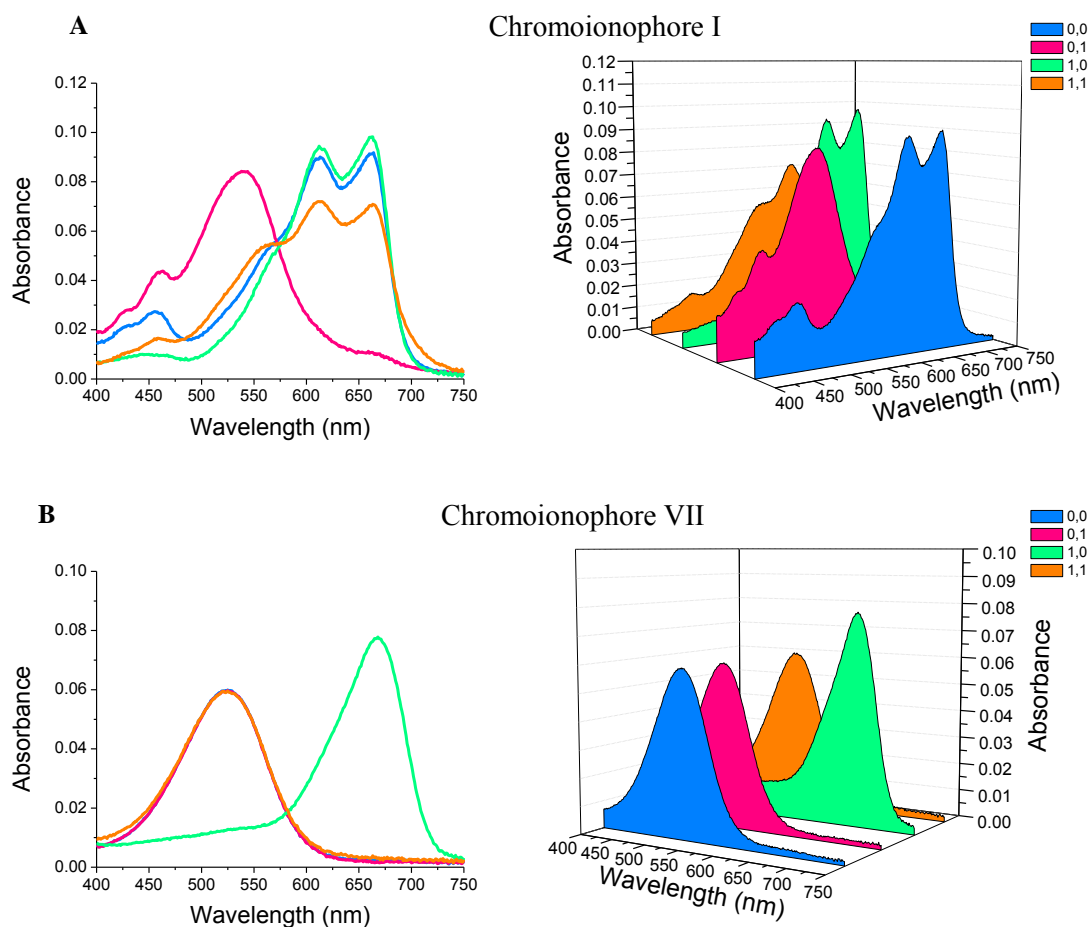


Figure 4.6. Absorbance features of the INH A/NINH A and INH B/NINH B gates of potassium optode of studied chromoionophores: (A) Chromoionophore I (1.0×10^{-2} M KNO_3 pH 4, pH 6) (B) Chromoionophore VII (1.0×10^{-1} M KNO_3 pH 4, pH 10) Input combination 0,0: blue; 0,1: pink; 1,0: green and 1,1: orange.

If we consider symbols of logic gates illustrated in Figure 4.7, an INH gate can turn to a AND gate by applying a NOT gate to the input A. Therefore, AND/NAND gates could be produced by switching proton input to an opposite logic condition to that employed in the case of the INH/NINH gate. The AND gate gave an output 1 only if both input A and input B are 1. Normally, logic value 0 of the input A was a high pH (H^+ concentration) while logic value 1 was a low pH. To obtain AND gate, logic value 0's condition of input A was swapped to be logic value 1, and vice versa. The combination 0,1 of INH A was changed to be combination (1,1) of AND logic gate. Strong absorbance at 540 nm (output O1) for chromoionophore I and Nile Blue-

urea optodes were found. The complement of this gate, NAND logic gate was also found in the output O2. Figure 4.8 and Table 4.3 shows absorbance features for all chromoionophores and truth table for AND/NAND logic gate.

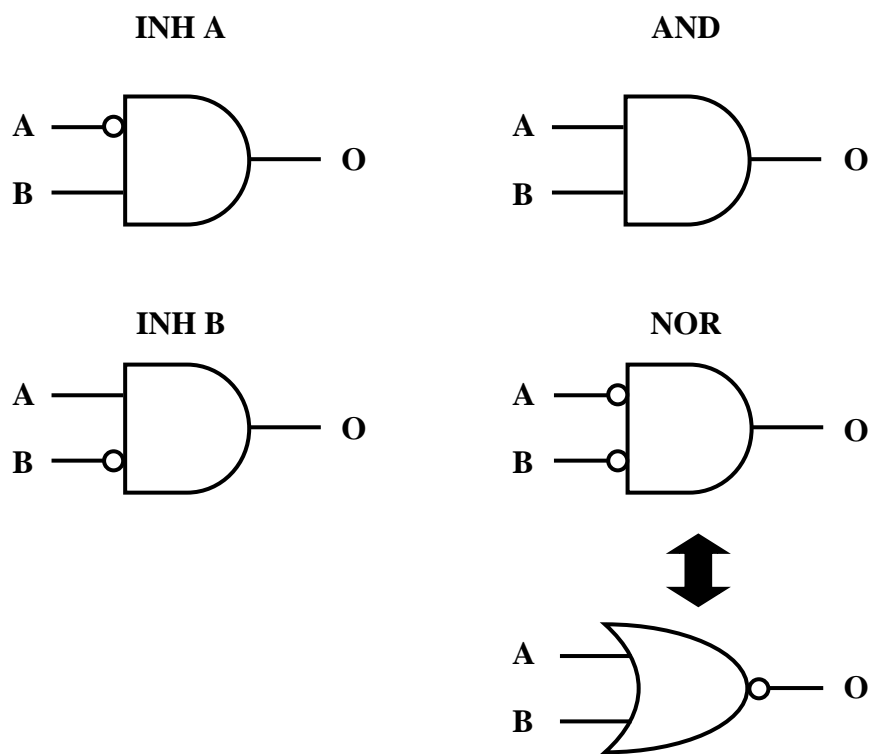


Figure 4.7. Symbol for INH A, INH B, AND and NOR gates.

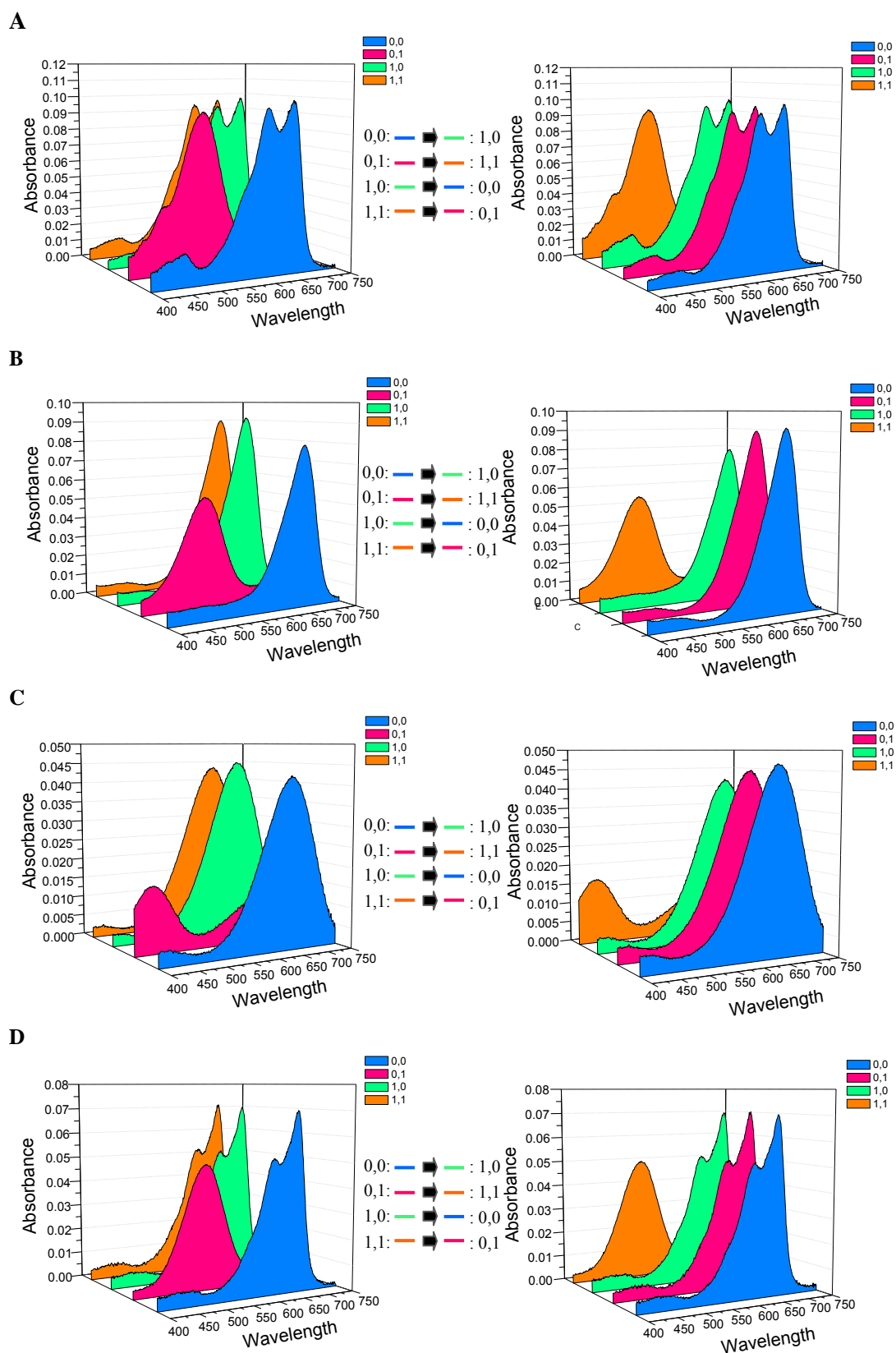


Figure 4.8. Interchanges from a INH A gate to a AND gate using (A) Chromoionophore I (1.0×10^{-1} M NaNO_3 pH 3, pH 7) (B) Chromoionophore VII

(1.0×10^{-2} M NaNO₃ pH 3, pH 6) (C) Chromoionophore XIV (1.0×10^{-3} M NaNO₃ pH 3, pH 5) (D) Nile Blue-urea (1.0×10^{-1} M NaNO₃ pH 3, pH 7) Input combination 0,0: blue; 0,1: pink; 1,0: green and 1,1: orange.

Table 4.5. Truth table corresponding to AND/NAND and OR/NOR gates

Input		Output			
A	B	AND	NAND	OR	NOR
0	0	0	1	0	1
0	1	0	1	1	0
1	0	0	1	1	0
1	1	1	0	1	0

A = H⁺ and B = Na⁺ or K⁺

Moreover, special OR/NOR gates were achieved from a INH B gate by applying a NOT gate to the input A as shown in Figure 4.7. A NOT gate was done by switching the pH condition of the input A to the opposite logic condition of INH B. The combination (1,0) of chromoionophore VII and XIV optodes that had a strong absorbance at 670 and 660 nm turns into combination (0,0). Then, the absorbance changes in Figure 4.9 for the OR/NOR were obtained.

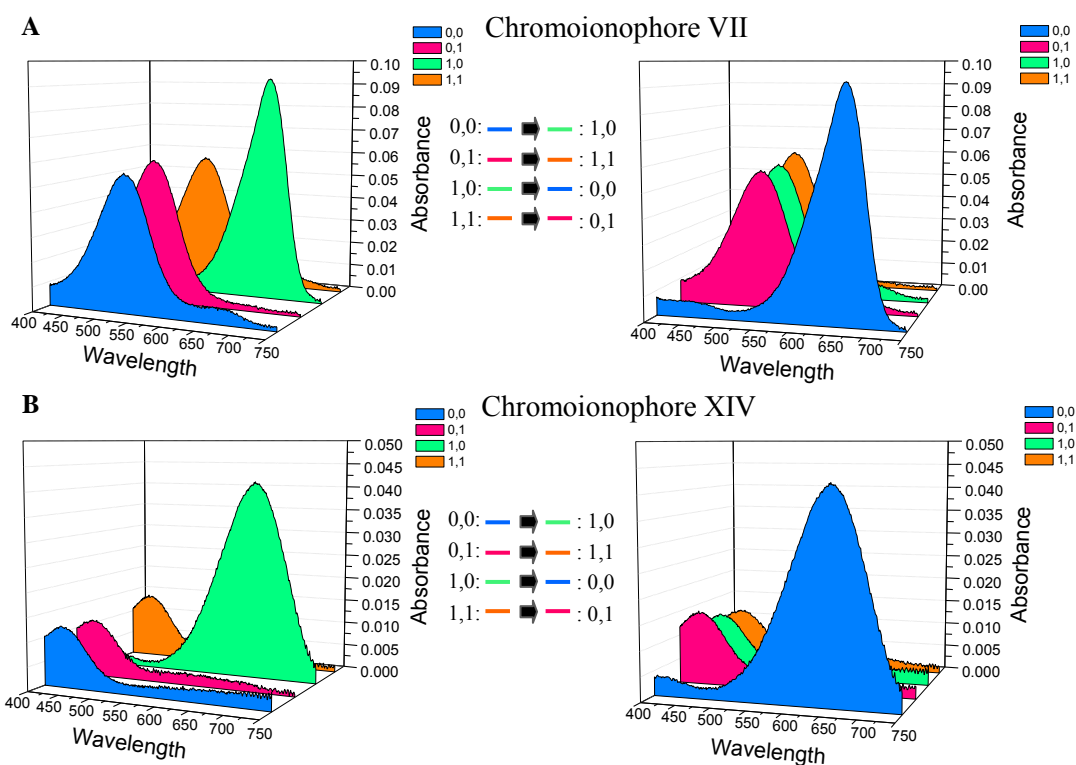


Figure 4.9. Interchanges from a INH B gate to an OR gate using (A) Chromoionophore VII (1.0×10^{-1} M NaNO_3 pH 5, pH 10) (B) Chromoionophore XIV (1.0×10^{-1} M NaNO_3 pH 5, pH 10) Input combination 0,0: blue; 0,1: pink; 1,0: green and 1,1: orange.

In addition, potassium optode also operates AND/NAND and OR/NOR logic gates in the same manner as sodium optode.

4.2 Mixed ionophore-2-primary ions

To tailor OR and NOR gates, a system composed of Na(X) and valinomycin as ionophores, Chromoionophore XIV or NB-urea as chromoionophore and sodium and potassium ions as input A and B, respectively was carried out. The output signal was the same absorbance of the chromoionophore as described previously. Upon the introduction of potassium ions in the system (input B in configuration 1), valinomycin in membrane phase could bind K^+ and the chromoionophore was then more deprotonated form. If sodium ion was added to the system (input A in configuration 1), or both input A and input B were introduced, the optode membrane gave the same

color change. Changes of absorbances were presented in Figure 4.10 and the respective truth table corresponding to the OR gate was given in Table 4.4. As a counterpart of the deprotonated λ_{\max} of chromoionophore (O1), the absorbance of output O2, protonated λ_{\max} of chromoionophore XIV and NB-urea at 660 and 665 nm, gave NOR gates. The threshold values for each gate were the same values as shown in Figure 4.5. The conditions that could operate OR/NOR gates were shown in Table 4.5.

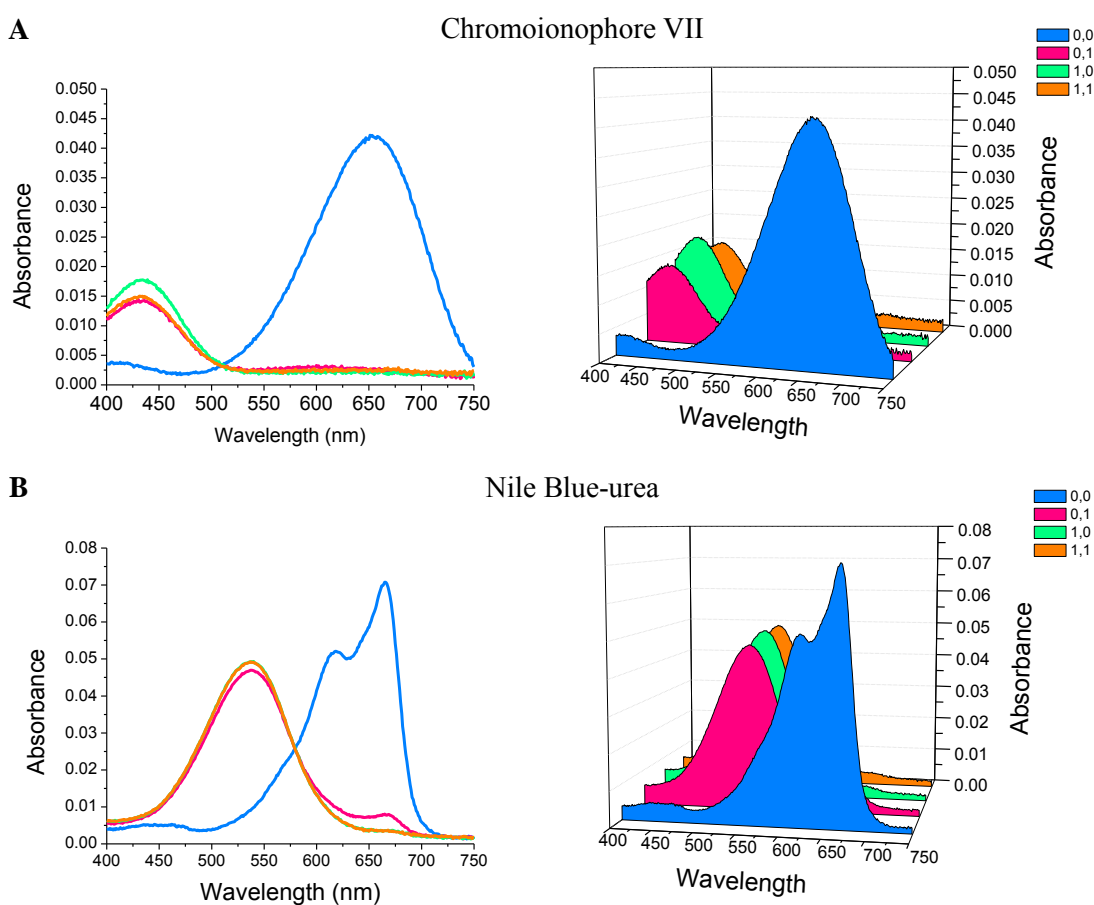


Figure 4.10. Absorbance features of OR and NOR gates using mixed ionophore strategy: (A) Chromoionophore XIV (pH 5.01) (B) Nile Blue-urea (pH 7.03). Input combination 0,0: blue; 0,1: pink; 1,0: green and 1,1: orange

Table 4.6. Truth table corresponding to OR/NOR gates

Input		Output	
A	B	OR	NOR
0	0	0	1
0	1	1	0
1	0	1	0
1	1	1	0

A = Na⁺ and B = K⁺

Table 4.7. pH value operated OR/NOR logic gates for mixed ionophore optode with sodium and potassium ions.

Chromoionophore	pH
Chromoionophore XIV	5, 6, 7
Nile Blue-urea	5, 6, 7, 8, 9,10

4.3 Mismatched ionophore-primary ion

In order to explore the application of optode logic gates, we studied responses of the optode films upon introducing a mismatched ion into the sample solution. Potassium ions were employed in the optode membrane containing Na(X) while sodium ions were used in the membrane composed of valinomycin. Although valinomycin did not interact well with sodium ions, Na(X) could somewhat bind with potassium ions. [82, 83]

Logic gates resulted from bulk optodes containing the mismatched ionophore are shown in Table 4.8. All chromoionophores produced INH and NINH gates in the same manner as matched ionophore-analyte ion optodes as a result of the same response mechanism. In Na(X)-Na⁺ and valinomycin-K⁺ systems, INH/NINH gates were obtained when metal concentration was high at low pH. If the pH was adjusted to be close to a working range of the pK_a of the chromoionophore, the optode membranes could produce INH/NINH gates in even low concentration of metal ions. In the Na(X)-K⁺ optode system, the ionophore did not complex well with potassium ion. Therefore, the complexation could not compete with binding of protons to chromoionophores. Logic gates from this system would be achieved in higher concentration of potassium ions and higher pH solution than typical optode systems.

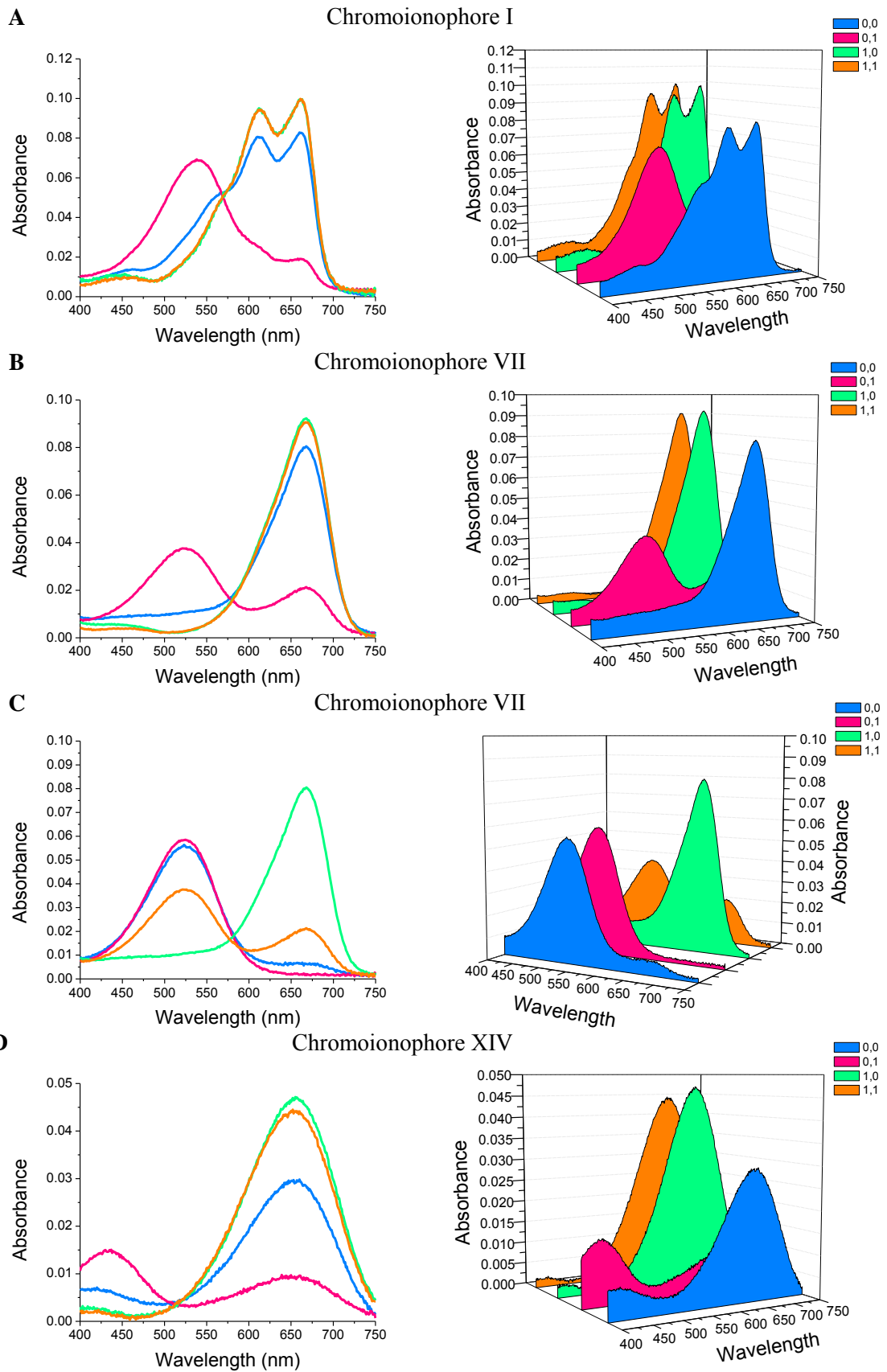
The absorbance features of the mismatched ionophore-primary ion were illustrated in Figure 4.11. If we compare Table 4.3 and Table 4.8, there were some conditions that were distinctively different conditions between the Na(X)-Na⁺ and Na(X)-K⁺ systems. These distinctive conditions were signified with the capital letters designating the chromoionophore as shown in Table 4.8. Condition C was found only at low pH values and high concentrations of K⁺ while D was found at high pH values and low concentrations of K⁺. For INH B gates, only C at high pH values and high concentrations of K⁺ will give such gates. Therefore, results in Table 4.8 could be possibly used to determine the predominant ion in solutions that contained Na⁺ and K⁺ or could be used to control the recognition and separation of such mixed ions.

Table 4.8. pH and metal concentration operated INH, NINH, AND, NAND, OR and NOR logic gates logic gates for sodium optode with potassium ion

pH ^a	INH/NINH A and AND/NAND ^b				INH/NINH B and OR/NOR ^b			
	Concentration of K ⁺ (M)				Concentration of K ⁺ (M)			
1,0	10 ⁻¹	10 ⁻²	10 ⁻³	10 ⁻⁴	10 ⁻¹	10 ⁻²	10 ⁻³	10 ⁻⁴
3,6	BC							
3,7	C	C						
3,8	d							
3,9	ad	d	d					
3,10	d	d	d	d				
4,6	B							
4,7	C	C						
4,8	d							
4,9	ad	d	d					
4,10	d	d	d	d				
5,7	C	C						
5,8	D							
5,9	AD	d	d					
5,10	D	d	d	d				
6,8	D				bc			
6,9	AD	D	d		bc			
6,10	D	D	d	d	bc			
7,9	A	D	D		C	C		
7,10		D	D	d	C	C		
8,10			D	D				

^a Input values of pH were alternated in the case of AND/NAND and OR/NOR gates.

^b a, b, c and d referred to chromoionophore I, VII, XIV and NB-urea, respectively. A, B, C and D also refer to chromoionophore I, VII, XIV and NB-urea, respectively but only found in Na(X)-K⁺ conditions.



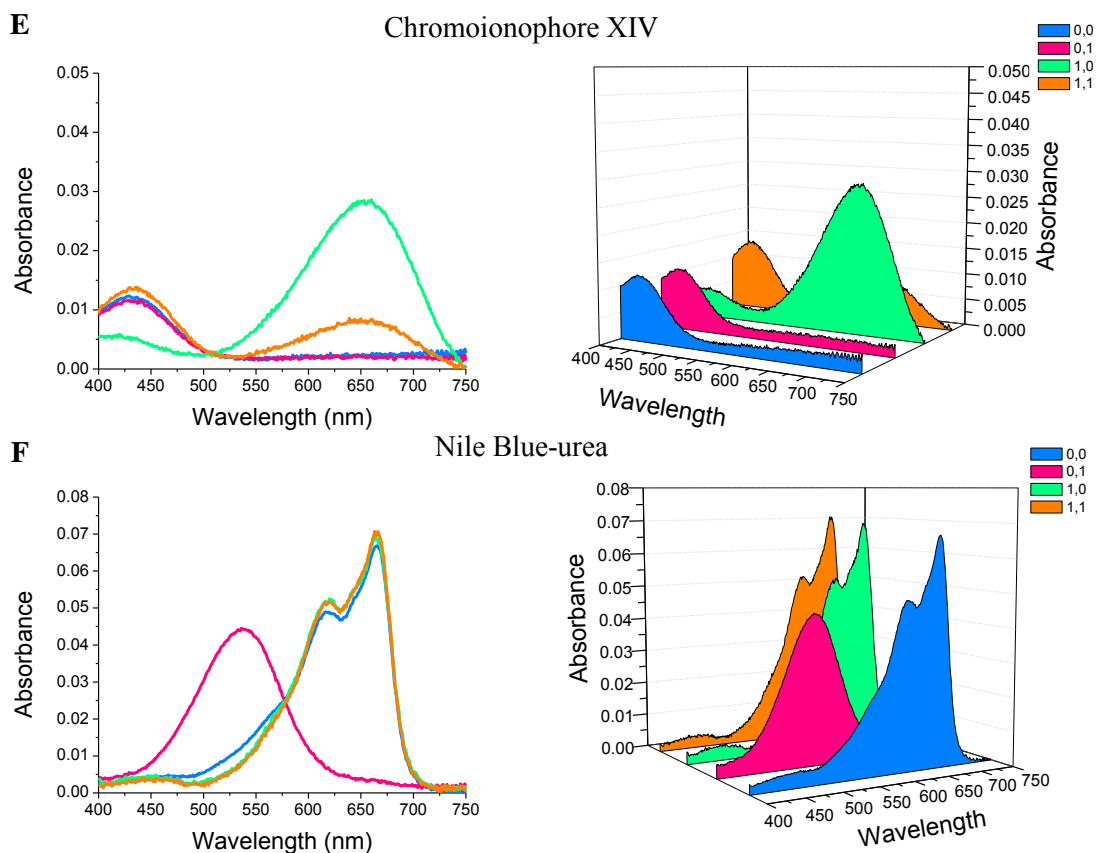


Figure 4.11. Absorbance features of the INH A/NINH A and INH B/NINH B gates of sodium optode with potassium ions of studied chromoionophores:

(A) Chromoionophore I (1.0×10^{-1} M NaNO_3 pH 3, pH 9) (B) Chromoionophore VII (1.0×10^{-1} M NaNO_3 pH 3, pH 6) (C) Chromoionophore VII (1.0×10^{-1} M NaNO_3 pH 6, pH 10) (D) Chromoionophore XIV (1.0×10^{-1} M NaNO_3 pH 3, pH 6) (E) Chromoionophore XIV (1.0×10^{-1} M NaNO_3 pH 6, pH 10) (F) Nile Blue-urea (1.0×10^{-1} M NaNO_3 pH 3, pH 9) Input combination 0,0: blue; 0,1: pink; 1,0: green and 1,1: orange.

The mismatched ionophore-primary ion also produced AND/NAND and OR/NOR logic gates similar to matched ionophore-primary ion case.

Sodium was the major positive ion in fluid outside of cells. Sodium regulated the total amount of water in the body and the transmission of sodium into and out of individual cells also played a role in critical body functions. Many processes in the body, especially in the brain, nervous system, and muscles, required electrical signals

for communication. The movement of sodium was critical in generation of these electrical signals. Potassium was the major positive ion found inside of cells. The proper level of potassium was essential for normal cell function. Among the many functions of potassium in the body were regulation of the heartbeat and the function of the muscles. Too much or too little sodium or potassium therefore could cause cells to malfunction, and extremes in the blood levels could be fatal. The bulk optode films could help determine the condition of electrolytes in the human body whether it was in the normal range by operating the logic gate absorbance from Table 4.8.

CHAPTER V

CONCLUSION

Our study has demonstrated that the optode membrane has been successfully applied to the construction of chemical logic gate operations. We have constructed the INH A, INH B, NINH A, NINH B, OR, NOR, AND and NAND logic gates. All logic gates operated by each optodes system were shown in Table 5.1. With a competition between H^+ and metal ion (Na^+ or K^+), two-input INH/NINH A and INH/NINH B logic gates were obtained depending on conditions of the inputs. By alternating the value of input H^+ , from '0' to '1' and vice versa, INH/NINH A would change to AND/NAND gates, and INH/NINH B would give OR/NOR gates. In addition, OR and NOR gates could be prepared using a mixed ionophore strategy (three-input logic operations). These gates might be reproduced in any other ion selective optodes due to their competitive ion exchange response mechanism.

Table 5.1 Logic gates derived from studied bulk optodes systems.

Ionophore	Input	Logic Gates
Na(X)	H^+, Na^+	INH A, INH B, NINH A, NINH B, AND, NAND, OR, NOR
Na(X)	H^+, K^+	INH A, INH B, NINH A, NINH B, AND, NAND, OR, NOR
Valinomycin	K^+	INH A, INH B, NINH A, NINH B, AND, NAND, OR, NOR
Na(X) + Valinomycin	Na^+, K^+	OR, NOR

We also demonstrated that bulk optode logic gates were possibly used for determining the predominant ion in mixed-ion solutions or controlling the recognition and separation of mixed ions. Our system can perhaps be used for information gathering as a miniaturized diagnostic system capable of working under physiological conditions.

Information systems based on wet molecular logic are likely to be applied increasingly in the medical sphere. In the mean time, simple logic operations are not just used in computers. As well as processing information, our system can be used for information gathering as a miniaturized diagnostic system capable of working under physiological conditions. Further investigation will enable us to evaluate the possibilities of implanted biocomputing devices to follow and transduce metabolic processes in the organism or readout drug delivery and therapeutic effectiveness through computational operations.

REFERENCES

- [1] Keyes, R.W. Fundamental limits of silicon technology. *Proceedings of the IEEE* 89 (3) (2001): 227-239.
- [2] Service, R.F. Can chemists assemble a future for molecular electronics? (News). *Science* 295 (2002): 2398.
- [3] Lipton, R.J. DNA solution of hard computational problems. *Science* 268 (5210) (1995): 542-544.
- [4] de Silva, P.A., Gunaratne, N.H.Q., and McCoy, C.P. A molecular photoionic AND gate based on fluorescent signaling. *Nature* 364 (6432) (1993): 42-44.
- [5] Aviram, A. Molecules for memory, logic, and amplification. *Journal of the American Chemical Society* 110 (17) (1988): 5687-5692.
- [6] de Silva, A.P., and Uchiyama, S. Molecular logic and computing. *Nature Nanotechnology* 2 (7) (2007): 399-410.
- [7] Pischel, U. Chemical Approaches to Molecular Logic Elements for Addition and Subtraction. *Angewandte Chemie International Edition* 46 (22) (2007): 4026-4040.
- [8] de Silva, A.P., Uchiyama, S., Vance, T.P., and Wannalser, B. A supramolecular chemistry basis for molecular logic and computation. *Coordination Chemistry Reviews* 251 (13-14) (2007): 1623-1632.
- [9] Credi, A. Molecules That Make Decisions. *Angewandte Chemie International Edition* 46 (29) (2007): 5472-5475.
- [10] Balzani, V., Credi, A., and Venturi, M. Molecular Logic Circuits. *ChemPhysChem* 4 (1) (2003): 49-59.
- [11] Szaciłowski, K., and Stasicka, Z. Molecular switches based on cyanoferrate complexes. *Coordination Chemistry Reviews* 229 (1-2) (2002): 17-26.
- [12] Wang, H., Zhang, D., Guo, X., Zhu, L., Shuai, Z., and Zhu, D. Tuning the fluorescence of 1-imino nitroxide pyrene with two chemical inputs: mimicking the performance of an "AND" gate. *Chemical Communications* (6) (2004): 670-671.
- [13] Uchiyama, S., McClean, G.D., Iwai, K., and de Silva, A.P. Membrane Media Create Small Nanospaces for Molecular Computation. *Journal of the American Chemical Society* 127 (25) (2005): 8920-8921.

- [14] Szaciłowski, K. Molecular Logic Gates Based on Pentacyanoferrate Complexes: From Simple Gates to Three-Dimensional Logic Systems. *Chemistry - A European Journal*, 10 (10) (2004): 2520-2528.
- [15] Magri, D.C., Brown, G.J., McClean, G.D., and de Silva, A.P. Communicating Chemical Congregation: A Molecular AND Logic Gate with Three Chemical Inputs as a “Lab-on-a-Molecule”• Prototype. *Journal of the American Chemical Society* 128 (15) (2006): 4950-4951.
- [16] Credi, A., Balzani, V., Langford, S.J., and Stoddart, J.F. Logic Operations at the Molecular Level. An XOR Gate Based on a Molecular Machine. *Journal of the American Chemical Society* 119 (11) (1997): 2679-2681.
- [17] Szaciłowski, K., Macyk, W., and Stochel, G.y. Light-Driven OR and XOR Programmable Chemical Logic Gates. *Journal of the American Chemical Society* 128 (14) (2006): 4550-4551.
- [18] de Sousa, M., de Castro, B., Abad, S., Miranda, M.A., and Pischel, U. A molecular tool kit for the variable design of logic operations (NOR, INH, EnNOR). *Chemical Communications* (19) (2006): 2051-2053.
- [19] de Silva, A.P., Dixon, I.M., Gunaratne, H.Q.N., Gunlaugsson, T., Maxwell, P.R.S., and Rice, T.E. Integration of Logic Functions and Sequential Operation of Gates at the Molecular-Scale. *Journal of the American Chemical Society* 121 (6) (1999): 1393-1394.
- [20] de Silva, A.P., James, M.R., McKinney, B.O.F., Pears, D.A., and Weir, S.M. Molecular computational elements encode large populations of small objects. *Nature Materials* 5 (10) (2006): 787-789.
- [21] Yoshizawa, M., Tamura, M., and Fujita, M. AND/OR Bimolecular Recognition. *Journal of the American Chemical Society* 126 (22) (2004): 6846-6847.
- [22] Wang, Z., Zheng, G., and Lu, P. 9-(Cycloheptatrienylydene)-fluorene Derivative: Remarkable Ratiometric pH Sensor and Computing Switch with NOR Logic Gate. *Organic Letters* 7 (17) (2005): 3669-3672.
- [23] Lee, S.H., Kim, J.Y., Kim, S.K., Lee, J.H., and Kim, J.S. Pyrene-appended calix[4]crowned logic gates involving normal and reverse PET: NOR, XNOR and INHIBIT. *Tetrahedron* 60 (24) (2004): 5171-5176.
- [24] Baytekin, H.T., and Akkaya, E.U. A Molecular NAND Gate Based on Watson-Crick Base Pairing. *Organic Letters* 2 (12) (2000): 1725-1727.
- [25] Zong, G., Xian, L., and Lu, G. L-Arginine bearing an anthrylmethyl group: fluorescent molecular NAND logic gate with H⁺ and ATP as inputs. *Tetrahedron Letters* 48 (22) (2007): 3891-3894.

- [26] Okamoto, A., Tanaka, K., and Saito, I. DNA Logic Gates. *Journal of the American Chemical Society* 126 (30) (2004): 9458-9463.
- [27] Hideaki, H., Nami, M., Kazuhiko, W., Eriko, N., Noriko, Y., and Koji, S. Ion sensing film optodes: disposable ion sensing probes for the determination of Na^+ , K^+ , Ca^{2+} and Cl^- concentrations in serum. *Sensors and Actuators B: Chemical* 29 (1-3) (1995): 378-385.
- [28] Morf, W.E., Seiler, K., Rusterholz, B., and Simon, W. Design of a novel calcium-selective optode membrane based on neutral ionophores. *Analytical Chemistry* 62 (7) (1990): 738-742.
- [29] Bakker, E., Lerchi, M., Rosatzin, T., Rusterholz, B., and Simon, W. Synthesis and characterization of neutral hydrogen ion-selective chromoionophores for use in bulk optodes. *Analytica Chimica Acta* 278 (2) (1993): 211-225.
- [30] Shortreed, M., Bakker, E., and Kopelman, R. Miniature Sodium-Selective Ion-Exchange Optode with Fluorescent pH Chromoionophores and Tunable Dynamic Range. *Analytical Chemistry* 68 (15) (1996): 2656-2662.
- [31] Xu, C., Qin, Y., and Bakker, E. Optical chloride sensor based on [9]mercuracarborand-3 with massively expanded measuring range. *Talanta* 63 (1) (2004): 180-184.
- [32] Wygladacz, K., Radu, A., Xu, C., Qin, Y., and Bakker, E. Fiber-Optic Microsensor Array Based on Fluorescent Bulk Optode Microspheres for the Trace Analysis of Silver Ions. *Analytical Chemistry* 77 (15) (2005): 4706-4712.
- [33] Bakker, E., Buhlmann, P., and Pretsch, E. Carrier-Based Ion-Selective Electrodes and Bulk Optodes. 1. General Characteristics. *Chemical Reviews* 97 (8) (1997): 3083-3132.
- [34] de Silva, A.P., and McClenaghan, N.D. Molecular-Scale Logic Gates. *Chemistry - A European Journal* 10 (3) (2004): 574-586.
- [35] Szaciłowski, K. Digital Information Processing in Molecular Systems. *Chemical Reviews* 108 (9) (2008): 3481-3548.
- [36] de Silva, A.P., Gunaratne, H.Q.N., and McCoy, C.P. Molecular Photoionic AND Logic Gates with Bright Fluorescence and "Off-On" Digital Action. *Journal of the American Chemical Society* 119 (33) (1997): 7891-7892.
- [37] Feynman, R. P. There's plenty of Room at the Bottom. *Engineering and Science* 23 (1960): 22-36.

- [38] Anelli, P.L., Ashton, P.R., Ballardini, R., Balzani, V., Delgado, M., Gandolfi, M.T., Goodnow, T.T., Kaifer, A.E., and Philp, D. Molecular meccano. 1.[2]Rotaxanes and a [2]catenane made to order. *Journal of the American Chemical Society* 114 (1) (1992): 193-218.
- [39] Huston, M.E., Akkaya, E.U., and Czarnik, A.W. Chelation enhanced fluorescence detection of non-metal ions. *Journal of the American Chemical Society* 111 (23) (1989): 8735-8737.
- [40] de Silva, A.P., de Siva, S.A., Dissanayake, A.S., and Sandanayake, K.R.A.S. Compartmental fluorescent pH indicators with nearly complete predictability of indicator parameters; molecular engineering of pH sensors. *Journal of the Chemical Society, Chemical Communications* 15 (1989): 1054-1056.
- [41] de Silva, A.P., and Sandanayake, K.R.A.S. Fluorescent PET (photo-induced electron transfer) sensors for alkali metal ions with improved selectivity against protons and with predictable binding constants. *Journal of the Chemical Society, Chemical Communications* 16 (1989): 1183-1185.
- [42] Hosseini, M.W., Blacker, A.J., and Lehn, J.M. Multiple molecular recognition and catalysis. A multifunctional anion receptor bearing an anion binding site, an intercalating group, and a catalytic site for nucleotide binding and hydrolysis. *Journal of the American Chemical Society* 112 (10) (1990): 3896-3904.
- [43] de Silva, A.P., Gunaratne, H.Q.N., and Maguire, G.L.N. "Off-On" Fluorescent Sensors for Physiological levels of Magnesium Ions based on photoinduced Electron Transfer (PET), which also behave as Photoionic OR Logic Gates. *Journal of the Chemical Society, Chemical Communications* (10) (1994): 1213-1214.
- [44] Gust, D., Moore, T.A., Moore, A.L., Gao, F., Luttrull, D., DeGraziano, J.M., Ma, X.C., Makings, L.R., and Lee, S.J. Long-lived photoinitiated charge separation in carotene-diporphyrin triad molecules. *Journal of the American Chemical Society* 113 (10) (1991): 3638-3649.
- [45] Ghosh, P., Bharadwaj, P.K., Mandal, S., and Ghosh, S. Ni(II), Cu(II), and Zn(II) Cryptate-Enhanced Fluorescence of a Trianthrylcryptand: A Potential Molecular Photonic OR Operator. *Journal of the American Chemical Society* 118 (6) (1996): 1553-1554.
- [46] Ghosh, P., Bharadwaj, P.K., Roy, J., and Ghosh, S. Transition Metal (II)/(III), Eu(III), and Tb(III) Ions Induced Molecular Photonic OR Gates Using Trianthryl Cryptands of Varying Cavity Dimension. *Journal of the American Chemical Society* 119 (49) (1997): 11903-11909.

- [47] McSkimming, G., Tucker, J.H.R., Bouas-Laurent, H., and Desvergne, J.-P. An Anthracene-Based Photochromic System That Responds to Two Chemical Inputs. *Angewandte Chemie International Edition* 39 (12) (2000): 2167-2169.
- [48] Cooper, C.R., and James, T.D. Synthesis and evaluation of D-glucosamine-selective fluorescent sensors. *Journal of the Chemical Society, Perkin Transactions 1* (6) (2000): 963-969.
- [49] Pina, F., Melo, M.J.o., Maestri, M., Passaniti, P., and Balzani, V. Artificial Chemical Systems Capable of Mimicking Some Elementary Properties of Neurons. *Journal of the American Chemical Society* 122 (18) (2000): 4496-4498.
- [50] Gobbi, L., Seiler, P., and Diederich, F. A Novel Three-Way Chromophoric Molecular Switch: pH and Light Controllable Switching Cycles. *Angewandte Chemie International Edition* 38 (5) (1999): 674-678.
- [51] Lukas, A.S., Bushard, P.J., and Wasielewski, M.R. Ultrafast Molecular Logic Gate Based on Optical Switching between Two Long-Lived Radical Ion Pair States. *Journal of the American Chemical Society* 123 (10) (2001): 2440-2441.
- [52] Remacle, F., Speiser, S., and Levine, R.D. Intermolecular and Intramolecular Logic Gates. *The Journal of Physical Chemistry B* 105 (24) (2001): 5589-5591.
- [53] Zhang, T., Zhang, C., Fu, G., Li, Y., Gu, L., Zhang, G., Song, Q.W., Parsons, B., and Birge, R.R. All-optical logic gates using bacteriorhodopsin films. *Optical Engineering* 39 (2) (2000): 527-534.
- [54] Miyaji, H., Kim, H.-K., Sim, E.-K., Lee, C.-K., Cho, W.-S., Sessler, J.L., and Lee, C.-H. Coumarin-Strapped Calix[4]pyrrole: A Fluorogenic Anion Receptor Modulated by Cation and Anion Binding. *Journal of the American Chemical Society* 127 (36) (2005): 12510-12512.
- [55] Gunnlaugsson, T., Donail, D.A.M., and Parker, D. Luminescent molecular logic gates: the two-input inhibit (INH) function. *Chemical Communications* (1) (2000): 93-94.
- [56] Gunnlaugsson, T., Mac Dónaill, D.n.A., and Parker, D. Lanthanide Macrocyclic Quinolyl Conjugates as Luminescent Molecular-Level Devices. *Journal of the American Chemical Society* 123 (51) (2001): 12866-12876.
- [57] Iwata, S., and Tanaka, K. A novel cation "AND" anion recognition host having pyrido[1',2':1,2]-imidazo[4,5-b]pyrazine as the fluorophore. *Journal of the Chemical Society, Chemical Communications* (15) (1995): 1491-1492.

- [58] Asakawa, M., Ashton, P.R., Balzani, V., Credi, A., Mattersteig, G., Matthews, O.A., Montalti, M., Spencer, N., Stoddart, J.F., and Venturi, M. Electrochemically Induced Molecular Motions in Pseudorotaxanes: A Case of Dual-Mode (Oxidative and Reductive) Dethreading. *Chemistry - A European Journal* 3 (12) (1997): 1992-1996.
- [59] Raymo, F.M. Digital Processing and Communication with Molecular Switches. *Advanced Materials* 14 (6) (2002): 401-414.
- [60] Leigh, D.A., Morales, M.Á.F., Pérez, E.M., Wong, J.K.Y., Saiz, C.G., Slawin, A.M.Z., Carmichael, A.J., Haddleton, D.M., Brouwer, A.M., Buma, W.J., Wurpel, G.W.H., León, S., and Zerbetto, F. Patterning through Controlled Submolecular Motion: Rotaxane-Based Switches and Logic Gates that Function in Solution and Polymer Films. *Angewandte Chemie International Edition* 44 (20) (2005): 3062-3067.
- [61] Alves, S., Pina, F., Albelda, M.T., García-España, E., Soriano, C., and Luis, S.V. Open-Chain Polyamine Ligands Bearing an Anthracene Unit - Chemosensors for Logic Operations at the Molecular Level. *European Journal of Inorganic Chemistry* 2001 (2) (2001): 405-412.
- [62] Rurack, K., Koval'chuck, A., Bricks, J.L., and Slominskii, J.L. A Simple Bifunctional Fluoroionophore Signaling Different Metal Ions Either Independently or Cooperatively. *Journal of the American Chemical Society* 123 (25) (2001): 6205-6206.
- [63] Seiler, K., and Simon, W. Principles and mechanisms of ion-selective optodes. *Sensors and Actuators B: Chemical* 6 (1-3) (1992): 295-298.
- [64] Morf, W.E., Seiler, K., Sørensen, P.R., and Simon, W. Ion-Selective Electrodes. Akadémiai Kiadó, Budapest, 1989.
- [65] Seiler, K., and Simon, W. Theoretical aspects of bulk optode membranes. *Analytica Chimica Acta* 266 (1) (1992): 73-87.
- [66] Suzuki, K., Ohzora, H., Tohda, K., Miyazaki, K., Watanabe, K., Inoue, H., and Shirai, T. Fibre-optic potassium ion sensors based on a neutral ionophore and a novel lipophilic anionic dye. *Analytica Chimica Acta* 237 (1990): 155-164.
- [67] Hisamoto, H., Watanabe, K., Nakagawa, E., Siswanta, D., Shichi, Y., and Suzuki, K. Flow-through type calcium ion selective optodes based on novel neutral ionophores and a lipophilic anionic dye. *Analytica Chimica Acta* 299 (2) (1994): 179-187.
- [68] Watanabe, K., Nakagawa, E., Yamada, H., Hisamoto, H., and Suzuki, K. Lithium ion selective optical fiber sensor based on a novel neutral ionophore and a lipophilic anionic dye. *Analytical Chemistry* 65 (19) (1993): 2704-2710.

- [69] Hisamoto, H., Watanabe, K., Oka, H., Nakagawa, E., Spichiger, U.E., and Suzuki, K. Flow-through type chloride ion selective optodes based on lipophilic organometallic chloride adducts and a lipophilic anionic dye. *Analytical Science* 10 (1994): 615-622.
- [70] Suzuki, K., Tohda, K., Tanda, Y., Ohzora, H., Nishihama, S., Inoue, H., and Shirai, T. Fiber-optic magnesium and calcium ion sensor based on a natural carboxylic polyether antibiotic. *Analytical Chemistry* 61 (4) (1989): 382-384.
- [71] Wolfbeis, O.S., and Schaffar, B.P.H. Optical sensors: An ion-selective optrode for potassium. *Analytica Chimica Acta* 198 (1987): 1-12.
- [72] Seiler, K., Wang, K., Bakker, E., Morf, W., Rusterholz, B., Spichiger, U., and Simon, W. Characterization of sodium-selective optode membranes based on neutral ionophores and assay of sodium in plasma. *Clinical Chemistry* 37 (8) (1991): 1350-1355.
- [73] Seiler, K., Morf, W.E., Rusterholz, B., and Simon, W. Design and characterization of a novel ammonium ion selective optical sensor based on neutral ionophores. *Analytical Science* 5 (1989): 557-561.
- [74] Kim, S.B., Cho, H.C., Cha, G.S., and Nam, H. Microtiter Plate-Format Optode. *Analytical Chemistry* 70 (22) (1998): 4860-4863.
- [75] Tsagkatakis, I., Peper, S., Retter, R., Bell, M., and Bakker, E. Monodisperse Plasticized Poly(vinyl chloride) Fluorescent Microspheres for Selective Ionophore-Based Sensing and Extraction. *Analytical Chemistry* 73 (24) (2001): 6083-6087.
- [76] Barker, S.L.R., Thorsrud, B.A., and Kopelman, R. Nitrite- and Chloride-Selective Fluorescent Nano-Optodes and in Vitro Application to Rat Conceptuses. *Analytical Chemistry* 70 (1) (1998): 100-104.
- [77] Clark, H.A., Hoyer, M., Philbert, M.A., and Kopelman, R. Optical Nanosensors for Chemical Analysis inside Single Living Cells. 1. Fabrication, Characterization, and Methods for Intracellular Delivery of PEBBLE Sensors. *Analytical Chemistry* 71 (21) (1999): 4831-4836.
- [78] Xu, C., Wygladacz, K., Qin, Y., Retter, R., Bell, M., and Bakker, E. Microsphere optical ion sensors based on doped silica gel templates. *Analytica Chimica Acta* 537 (1-2) (2005): 135-143.
- [79] Ngeontae, W., Xu, C., Ye, N., Wygladacz, K., Aeungmaitrepirom, W., Tuntulani, T., and Bakker, E. Polymerized Nile Blue derivatives for plasticizer-free fluorescent ion optode microsphere sensors. *Analytica Chimica Acta* 599 (1) (2007): 124-133.

- [80] Qin, Y., and Bakker, E. Quantitative binding constants of H⁺-selective chromoionophores and anion ionophores in solvent polymeric sensing membranes. *Talanta* 58 (5) (2002): 909-918.
- [81] O'Neill, S., Conway, S., Twellmeyer, J., Egan, O., Nolan, K., and Diamond, D. Ion-selective optode membranes using 9-(4-diethylamino-2-octadecanoatestyryl)-acridine acidochromic dye. *Analytica Chimica Acta* 398 (1) (1999): 1-11.
- [82] Arnaud-Neu, F., Collins, E.M., Deasy, M., Ferguson, G., Harris, S.J., Kaitner, B., Lough, A.J., McKervey, M.A., and Marques, E. Synthesis, x-ray crystal structures, and cation-binding properties of alkyl calixaryl esters and ketones, a new family of macrocyclic molecular receptors. *Journal of the American Chemical Society* 111 (23) (1989): 8681-8691.
- [83] Varma, S., Sabo, D., and Rempe, S.B. K⁺/Na⁺ Selectivity in K Channels and Valinomycin: Over-coordination Versus Cavity-size constraints. *Journal of Molecular Biology* 376 (1) (2008): 13-22.
- [84] Shiva, S.G. Introduction to Logic Design. 2nd Ed., CRC Press, 1998.
- [85] Rafiquzzaman, M. Fundamentals of Digital Logic and Microcomputer Design. John Wiley & Sons, Inc., 2005.

APPENDICES

Appendix A

Digital System Organization [84]

We are surrounded today by a myriad of digital devices. Digital watches, electronic calculators, digital meters, microprocessors and digital computers are all examples of such systems. A *digital system* manipulates data that are composed of a finite number of discrete elements. Results that the digital produce are also made up of a set of discrete elements. In contrast, an *analog system* manipulates data that are represented in a continuous form, producing results that also appear in continuous form. Figure 1 shows the components of a digital computer, the most general digital device. The program to manipulate the data is first brought into the *memory unit* through the *input device*. The data to be processed are then brought into the memory unit, also through the input device. The *control unit* fetches instructions from the program stored in the memory one at a time, analyzes each instruction, and instructs the *processing unit* to perform the operations called for by the instruction. The results produced by the processing unit are forwarded to the memory unit for storage and then transferred to the *output device*.

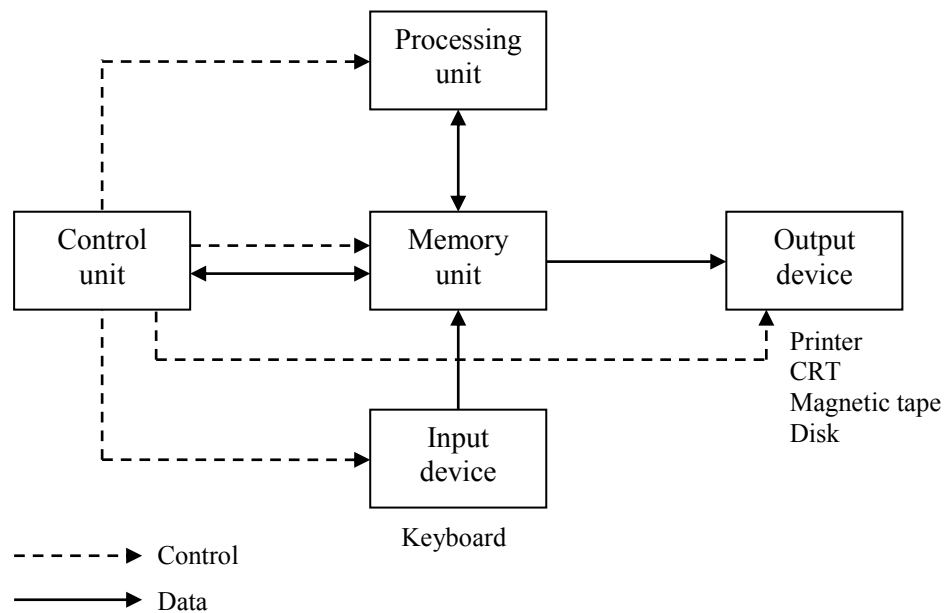


Figure A1. Components of a digital computer.

Digital systems typically use a two level representation, with one voltage level representing a 0 and the other representing a 1. To represent all 10 decimal digits using this binary-(two-valued) alphabet of 0 and 1, a unique pattern of 0s and 1s is assigned to each digit. Because the data elements and operations are all represented in binary form in all practical digital systems, a good understanding of the binary number system and data representation is basic to the analysis and design of digital system hardware.

Appendix B

Logic Gates [85]

A logic gate performs a logical operation on one or more logic inputs and produces a single logic output. Because the output is also a logic-level value, an output of one logic gate can connect to the input of one or more other logic gates. The logic normally performed is Boolean logic and is most commonly found in digital circuits. A digital system is where the input and output only involves two levels of voltage, high (1) or low (0).

Table B1. The other names for the logic level.

Logic Level	
1	0
True	False
On	Off
+Vs	-Vs
+Vs	Gnd
Open	Closed

The logic gates are called „gates“ because they give a „1“ on the output only when a particular combination of 0 and 1 is present at the inputs. This „input“ is the key to open the gate which is the output.

1) Logic Gate Symbols

The IEEE standard provides two different types of symbols for logic gates. One type, called *distinctive-shape symbols*, is what we have been using all along. The other type, called *rectangular-shape symbols*, uses the same shape for all the gates, along with an internal label to identify the type of gate. Figure 2.2 compares the two types. Before the promulgation of the IEEE standard, logic symbols for larger

scale logic elements were drawn in an ad hoc manner; the only standard rule was to use rectangles with inputs on the left and outputs on the right.


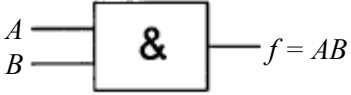
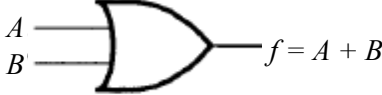
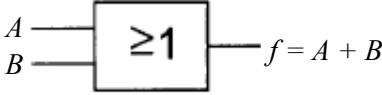

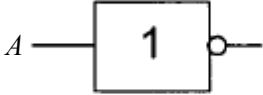
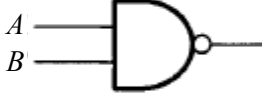
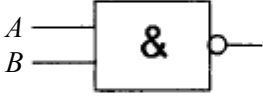
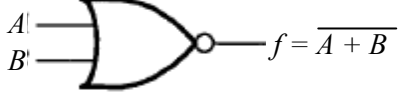
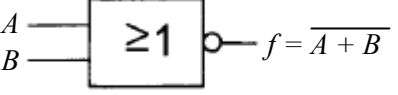
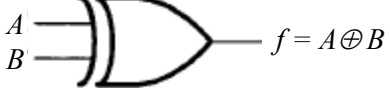
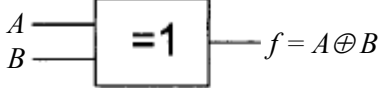
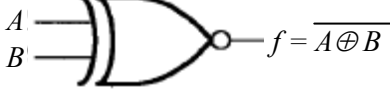
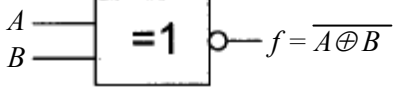
Gate	Common Symbol	IEEE Symbol
AND		
OR		
NOT		
NAND		
NOR		
Exclusive-OR		
Exclusive-NOR		

Figure B1. Symbols for logic gates

2) Logic Operations

Boolean algebra used three basic logic operations namely, NOT, OR, and AND. These operations are described in the following section.

NOT operation

The NOT operation inverts or provides the ones complement of a binary digit, This operation takes a single input and generates one output. The NOT operation of a binary digit provides the following result:

$$\text{NOT } 1 = 0 \quad \text{NOT } 0 = 1$$

Therefore, NOT of a Boolean variable A , written as \bar{A} (or A') is 1 if and only if A is 0. Similarly, \bar{A} is 0 if and only if A is 1. The symbolic representation of an electronic circuit that implements a NOT operation is shown in Figure 2.3. A NOT gate is also referred to as an “inverter” because it inverts the voltage levels.

OR operation

The OR operation for two variables A and B generates a result of 1 if A or B , or both, are 1. However, if both A and B are zero, then the result is 0.

A plus sign $+$ (logical sum) or \vee symbol is normally used to represent OR. The four possible combinations of OR for two binary digits are

$$\begin{aligned} 0 + 0 &= 0 \\ 0 + 1 &= 1 \\ 1 + 0 &= 1 \\ 1 + 1 &= 1 \end{aligned}$$

AND operation

The AND operation for two variables A and B generates a result of 1 if both A and B are 1. However, if either A or B , or both, are zero, then the result is 0.

The dot \cdot and \wedge symbol are both used to represent the AND operation. The AND operation between two binary digits is

$$\begin{aligned} 0 \cdot 0 &= 0 \\ 0 \cdot 1 &= 0 \\ 1 \cdot 0 &= 0 \\ 1 \cdot 1 &= 1 \end{aligned}$$

Because these three gates alone are not sufficient to perform all the necessary logic functions, combinational logic circuits that obey different truth tables can be assembled connecting NOT, OR, and AND gates. The six other important logic operations are NOR, NAND, Exclusive-OR (XOR), Exclusive-NOR (XNOR), Inhibit (INH) and Non-inhibit (NINH).

NOR operation

The NOR output is produced by inverting the output of an OR operation, as shown by the small circle at the output. A NOR gate can have two or more inputs, its output is true if no inputs are true.

NAND operation

The NAND output is generated by inverting the output of an AND operation. A NAND gate can have two or more inputs. Its output is true if NOT all inputs are true.

Exclusive-OR operation (XOR)

The Exclusive-OR operation (XOR) generates an output of 1 if the inputs are different and 0 if the inputs are the same. The \oplus or \vee symbol is used to represent the XOR operation. The XOR operation between binary digits is

$$\begin{aligned} 0 \oplus 0 &= 0 \\ 0 \oplus 1 &= 1 \\ 1 \oplus 0 &= 1 \\ 1 \oplus 1 &= 0 \end{aligned}$$

$A \oplus B$ is 1 only when $A=0$ and $B=1$ or $A=1$ and $B=0$. Therefore,

$$C = A \oplus B = \bar{A}B + A\bar{B}$$

This is like an OR gate but excluding both inputs being true. The output is true if input A and B are different.

Exclusive-NOR Operation (XNOR)

The one's complement of the Exclusive-OR operation is known as the Exclusive-NOR operation. The XNOR operation is represented by the symbol \odot . Therefore, $C = \overline{A \oplus B} = A \odot B$. The XNOR operation is also called equivalence. From the truth table, output C is 1 if both A and B are 0's or both A and B are 1's; otherwise C is 0. That is, $C = 1$, for $A = 0$ and $B = 0$ or $A = 1$ and $B = 1$. Hence, $C = A \odot B = \bar{A}\bar{B} + AB$.

INH operation

An Inhibit (INH) logic gate is basically AND gates with one of the inputs inverted through a NOT function.

NINH operation

The Non-Inhibit (NINH) output is produced by inverting the output of and INH operation.

Note that the symbol C is chosen arbitrarily in all the above logic operations to represent the output of each logic gate. Also, note that all logic gates (except NOT) can have at least two inputs with only one output. The NOT gate, on the other hand, has one input and one output.

3) Truth Tables for Logic Gates

A truth table is used to record all the possible combinations of inputs and the corresponding output decisions for a particular logic. The behavior of the logic circuit can be summarized by a truth table. In a truth table, the input and output states are represented by the binary numbers 0 or 1. The operation of the Boolean algebra can be shown in Table B2.

Table B2. Truth tables for two input logic gates.

Input		Output							
		OR	AND	XOR	INH	NOR	NAND	XNOR	NINH
0	0	0	0	0	0	1	1	1	1
0	1	1	0	1	1	0	1	0	0
1	0	1	0	1	0	0	1	0	1
1	1	1	1	0	0	0	0	1	1

Appendix C

Boolean Algebra [86]

In 1854 George Boole introduced a symbolic notation to deal with logic statements that take a value of “true” or “false.” This notation has come to be known as Boolean algebra. Boolean algebra provides basis for logic operations using binary variables. Alphabetic characters are used to represent the binary variables. A binary variable can have either true or complement value. For example, the binary variable A can be either and/or \bar{A} in a Boolean function.

A Boolean function is an operation expressing logical operation between binary variables. The Boolean function can have a value of 0 or 1. As an example of a Boolean function, consider the following:

$$f = \bar{A}\bar{B} + C$$

Here, the Boolean function f is 1 if both \bar{A} and \bar{B} are 1 or C is 1; otherwise f is 0. Note that \bar{A} means that if $A = 1$, then $\bar{A} = 0$. Thus, when $B = 1$, then $\bar{B} = 0$. It can therefore be concluded that f is one when $A = 0$ and $B = 0$ or $C = 1$.

A truth table can be used to represent a Boolean function. The truth table contains a combination of 1’s and 0’s for the binary variables. Furthermore, the truth table provides the value of the Boolean function as 1 or 0 for each combination of the input binary variables. A Boolean function can also be represented in terms of a logic diagram. Figure 2.3 shows the logic diagram for $f = \bar{A}\bar{B} + C$.

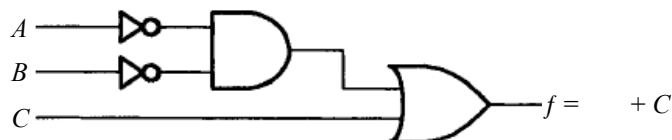


Figure C1. Logic diagram for $f = \bar{A}\bar{B} + C$

$= B + A$ (commutative) and $(A + B) + C = A + (B + C)$ (associative). This means that the OR gate inputs can be interchanged. Thus, the OR gate can have more than two inputs. Similarly, using the identities 6b and 7b, it can be shown that the AND gate can also have more than two inputs. Note that the NOR and NAND operations, on the other hand, are commutative, but not associative. Therefore, it is not possible to have NOR and NAND gates with more than two inputs. However, NOR and NAND gates with more than two inputs can be obtained by using inverted OR and inverted AND respectively. The Exclusive-OR and Exclusive-NOR operations are both commutative and associative. Thus, these gates can have more than two inputs. However, Exclusive-OR and Exclusive-NOR gates with more than two inputs are uncommon from a hardware point of view.

Appendix D

Threshold Value for Absorbance Output Calculation

The value chosen for 1 or 0 represents the difference between the corresponding spectra. Threshold values are determined by fix degree of deprotonation (α) at 0.6. The measured absorbance A at a given equilibrium can be related to α by measuring the absorbances of the fully protonated (A_P) and nonprotonated form (A_D) of the chromoionophore:

$$\alpha = \frac{A_P - A}{A_P - A_D}$$

Table D1. Wavelength for outputs O1 and O2

Chromoionophore	Wavelength for output O1 absorbance (nm)	Wavelength for output O2 absorbance (nm)
Chromoionophore I	540	665
Chromoionophore VII	530	670
Chromoionophore XIV	435	660
Nile Blue-urea	540	665

Chromoionophore I

Threshold value for output O1 (540 nm):

$$A_D = 0.0957 \quad A_P = 0.0256$$

$$A = A_D - (A_D - A_P) \alpha$$

$$A = 0.0957 - (0.0957 - 0.0256) \times 0.6$$

$$A = 0.0536$$

Threshold value for output O2 (665 nm):

$$A_D = 0.0979 \quad A_P = 0.0018$$

$$A = A_P - (A_P - A_D) \alpha$$

$$A = 0.0018 - (0.0018 - 0.0979) \times 0.6$$

$$A = 0.0402$$

Chromoionophore VII

Threshold value for output O1 (530 nm):

$$A_D = 0.0584 \quad A_P = 0.0039$$

$$A = A_D - (A_D - A_P) \alpha$$

$$A = 0.0584 - (0.0584 - 0.0039) \times 0.6$$

$$A = 0.0257$$

Threshold value for output O2 (670 nm):

$$A_D = 0.0921 \quad A_P = 0.0021$$

$$A = A_P - (A_P - A_D) \alpha$$

$$A = 0.0921 - (0.0921 - 0.0021) \times 0.6$$

$$A = 0.0381$$

Chromoionophore XIV

Threshold value for output O1 (435 nm):

$$A_D = 0.0253 \quad A_P = 0.0033$$

$$A = A_D - (A_D - A_P) \alpha$$

$$A = 0.0253 - (0.0253 - 0.0033) \times 0.67$$

$$A = 0.0105$$

Threshold value for output O2 (660 nm):

$$A_D = 0.0463 \quad A_P = 0.0017$$

$$A = A_P - (A_P - A_D) \alpha$$

$$A = 0.0463 - (0.0463 - 0.0017) \times 0.6$$

$$A = 0.0195$$

Nile Blue-urea

Threshold value for output O1 (540 nm):

$$A_D = 0.0528 \quad A_P = 0.0098$$

$$A = A_D - (A_D - A_P) \alpha$$

$$A = 0.0528 - (0.0528 - 0.0098) \times 0.6$$

$$A = 0.0270$$

Threshold value for output O2 (665 nm):

$$A_D = 0.0696 \quad A_P = 0.0015$$

$$A = A_P - (A_P - A_D) \alpha$$

$$A = 0.0696 - (0.0696 - 0.0015) \times 0.6$$

$$A = 0.0287$$

Appendix E

Details of Non-Logic Gate Operations

Table E1. Truth table for non-logic gates X/X^{''} and Y/Y^{''}

Input A H ⁺	Input B Na ⁺	X	X ^{''}	Y	Y ^{''}
0	0	1	0	0	1
0	1	0	1	0	1
1	0	1	0	1	0
1	1	0	1	1	0

Table E2. pHs and metal concentrations which operated X, X^{''}, Y, and Y^{''} logic gates for Na⁺ and K⁺ selective bulk optodes

pH 1,0	X/X ^{''a,b,c} Concentration of Na ⁺ (M)				Y/Y ^{''a,b,c} Concentration of Na ⁺ or K ⁺ (M)			
	10 ⁻¹	10 ⁻²	10 ⁻³	10 ⁻⁴	10 ⁻¹	10 ⁻²	10 ⁻³	10 ⁻⁴
3,5	C							
3,6	C							
3,7							C	C
3,8					bc	Bbc	BCbc	BCbc
3,9					bc	Bbc	BCbc	BCbc
3,10					bc	Bbc	BCbc	BCbc
4,6	BC	C						
4,8					b	bc	Bbc	BCbc
4,9					b	bc	BCbc	BCbc
4,10					b	bc	bc	Bc
5,8					bc	bc	bc	Bbc
5,9					bc	bc	bc	Bbc
5,10					bc	bc	bc	Bbc
6,8	AD						bc	bc
6,9	AD						bc	bc
6,10	D						bc	bc
7,9	AD	AD					c	c
7,10	D	D						c
8,10	Dd	D	D	D				

^aA, B, C and D referred to chromoionophores I, VII, XIV and Nile Blue-urea, respectively in sodium optode.

^ba, b, c and d referred to chromoionophores I, VII, XIV and Nile Blue-urea, respectively in potassium optode.

^cX^{''} and Y^{''} operations were obtained from output O2 of the chromoionophores.

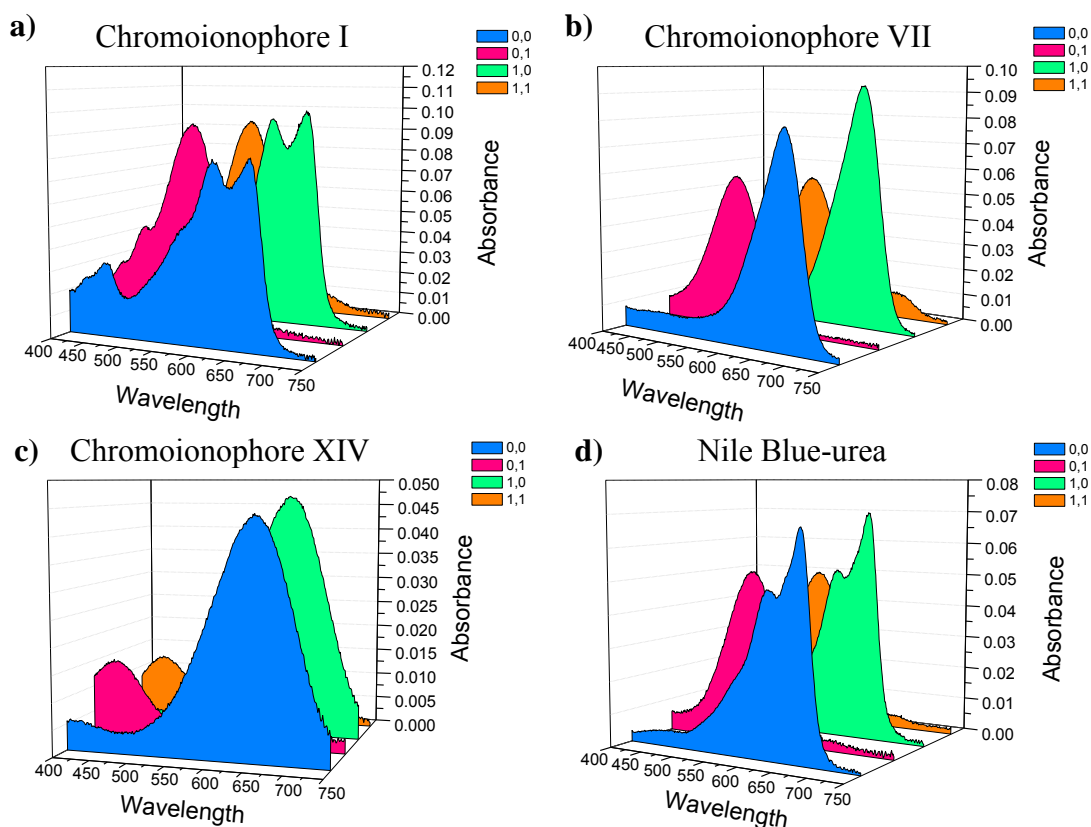


Figure E1. Absorbance features of the X and X'' of sodium optode of studied chromoionophores: (a) Chromoionophore I (10^{-1} M NaNO_3 pH6, pH8) (b) Chromoionophore VII (10^{-1} M NaNO_3 pH3, pH5) (c) Chromoionophore XIV (10^{-1} M NaNO_3 pH3, pH5) (d) Nile Blue-urea (10^{-1} M NaNO_3 pH6, pH8) Input combination 0,0: blue; 0,1: pink; 1,0: green and 1,1: orange.

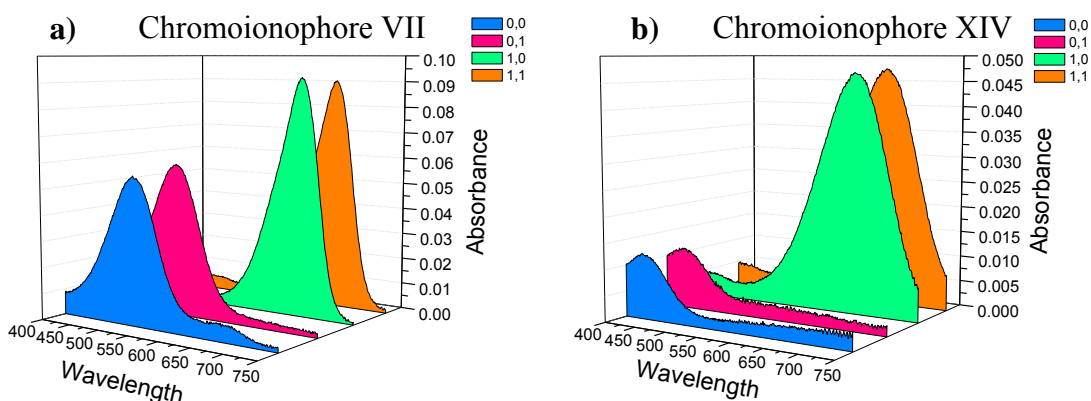


Figure E2. Absorbance features of the Y and Y'' of sodium optode of studied chromoionophores: (a) Chromoionophore VII (10^{-3} M NaNO_3 pH4, pH6) (b)

Chromoionophore XIV (10^{-3} M NaNO₃ pH3, pH7) Input combination 0,0: blue; 0,1: pink; 1,0: green and 1,1: orange.

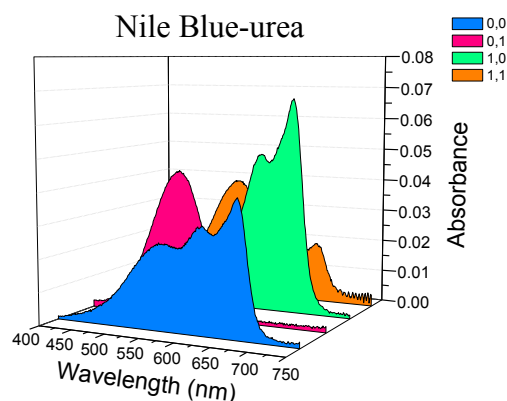


Figure E3. Absorbance features of the X and X'' of potassium optode of studied Chromoionophores I (10^{-1} M NaNO₃ pH8, pH10) Input combination 0,0: blue; 0,1: pink; 1,0: green and 1,1: orange.

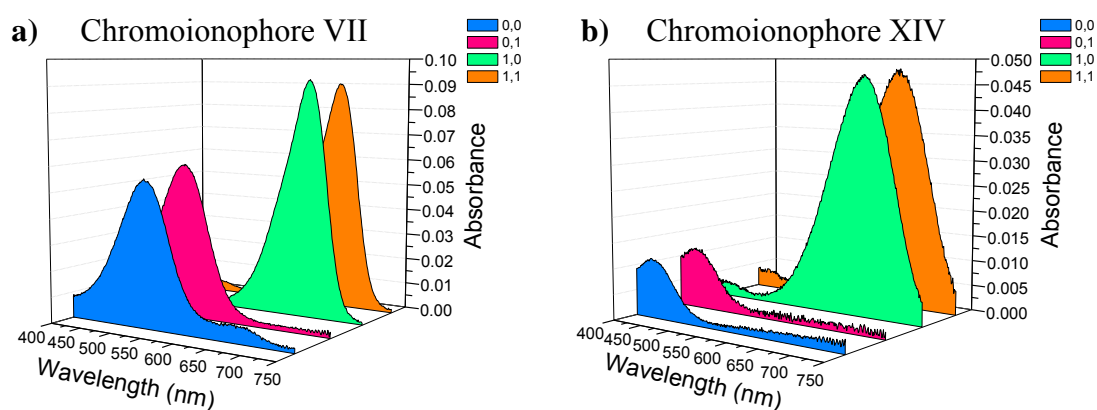


Figure E4. Absorbance features of the Y and Y'' of potassium optode of studied chromoionophores: (a) Chromoionophore VII (10^{-1} M NaNO₃ pH3, pH8) (b) Chromoionophore XIV (10^{-1} M NaNO₃ pH3, pH8) Input combination 0,0: blue; 0,1: pink; 1,0: green and 1,1: orange.

VITA

Miss Dhassida Sooksawat was born on March 5, 1985 in Songkhla, Thailand. She has got the scholarship from the Development and Promotion of Science and Technology Talent Project (DPST) since 2000. After completing her secondary school from Hatyai Wittayalai School, she entered the Department of Chemistry, Faculty of Science, Prince of Songkla University in 2003. She received her Bachelor of Science Degree in March 2007 with first class honor. She then continued her graduate study at Chulalongkorn University and worked in Inorganic Chemistry, then become a member of Supramolecular Chemistry Research Unit.